Hydrocarbon C−H Bond Activation by a Tungsten Acetylene Complex

Jeff D. Debad,[†] Peter Legzdins,*[,†] Sean A. Lumb,[†] Steven J. Rettig,[†,§] Raymond J. Batchelor,[‡] and Frederick W. B. Einstein[‡]

Department of Chemistry, The University of British Columbia, Vancouver, British Columbia, Canada V6T 1Z1, and the Department of Chemistry, Simon Fraser University, Burnaby, British Columbia, Canada V5A 1S6

Received June 9, 1999

Thermal activation of Cp*W(NO)(η^2-CPhCH$_2$)(CH$_2$SiMe$_3$) (**1**) in neat hydrocarbon solutions transiently generates Cp*W(NO)(η^2-PhC≡CH) (**A**), which subsequently activates solvent C−H bonds. For example, the thermolysis of **1** in benzene solution generates quantitatively Cp*W(NO)(η^2-CPhCH$_2$)(Ph) (**2**). The thermolysis of **1** in solutions of methyl-substituted arenes such as toluene or *p*-, *m*-, or *o*-xylene provides mixtures of aryl and benzyl vinyl complexes of the general formulas Cp*W(NO)(η^2-CPhCH$_2$)(aryl), Cp*W(NO)(η^2-CPhCH$_2$)(η^1-benzyl), or Cp*W(NO)(η^2-benzyl)(η^1-CPh=CH$_2$). Similarly, the thermolysis of **1** in (Me$_3$Si)$_2$O affords Cp*W(NO)(η^2-CPhCH$_2$)(CH$_2$SiMe$_2$OSiMe$_3$) (**10**). Mechanistic and kinetic studies support the proposal that the formation of **A** from **1** by elimination of silane is the rate-controlling process in these reactions. Intra- and intermolecular selectivity studies reveal that the strongest C−H bond (yielding the stronger M−C bond) is the preferred site of reactivity, as expected. Dual C−H bond activation of aliphatic hydrocarbons occurs during the thermal activation of **1** in solutions of these substrates. Consequently, metallacycles of the form Cp*W(NO)(η^2-*C*H(η^2-Ph)CH$_2$CH(R)*C*H$_2$) [(**11**) R = ^{n}Pr; (**12**) R = ^{n}Bu; (**13**) R = ^{t}Bu; and (**14**) R = OEt] result from the dehydrogenation of *n*-pentane, *n*-hexane, 2,2-dimethylbutane, and diethyl ether, respectively. This dual C−H activation process displays a selectivity for substrates that contain an ethyl substituent. Dual C−H bond activation of 2,3-dimethyl-2-butene in the presence of **1** under thermolysis conditions regioselectively affords Cp*W(NO)(η^3-*endo*-CH$_2$C(Me)C(Me)CH$_2$(η^1-CPhMe)) (**15**). Attempts to trap acetylene complex **A** with PMe$_3$ result in the formation of the metallacyclopropane complex Cp*W(NO)(CH$_2$SiMe$_3$)(η^2-CH$_2$CPh(PMe$_3$)) (**16**). All new complexes have been characterized by conventional spectroscopic methods, and the solid-state molecular structures of compounds **11**, **15**, and **16** have been established by X-ray diffraction methods.

Introduction

There exist two main thrusts in the study of hydrocarbon C−H bond activation by organometallic complexes if the ultimate goal in this field is the conversion of hydrocarbon feedstocks into more elaborate, functionalized, or utilizable organic compounds. The first is the systematic investigation of transition metal systems capable of activating hydrocarbon C−H bonds, with a view toward understanding the physicochemical requirements of this mode of reactivity. Toward this end, extensive studies of C−H bond activation by metal complexes of nearly every group in the transition series, in addition to complexes of the lanthanides and actinides, have greatly expanded our understanding of the various mechanisms of C−H bond activation.[1]

Equally important, the second goal toward the derivatization of hydrocarbons requires the application of this amassed knowledge to the design of systems capable not only of C−H activation but also of chemical elaboration of the resultant hydrocarbyl fragment. At present the reactivity of many previously studied systems ceases following the C−H activation event, often as a result of the limitations imposed by the metal's valence-electron shell during the activation process. C−H bond activation frequently occurs at electronically unsaturated metal centers in intermediates generated from saturated or kinetically stable precursors. Cleavage of a hydrocarbyl C−H bond then results in the regeneration of a stable, coordinatively saturated metal center at which no further chemistry can occur. In a few cases, however, further reactivity occurs beyond the C−H activation event, resulting in (for example) dehydrogenation of the alkane to an alkene[2] or hydroformy-

[†] The University of British Columbia.
[‡] Simon Fraser University.
[§] Deceased October 27, 1998.

(1) This field has been extensively reviewed. See, for example: (a) Shilov, A. E.; Shul'pin, G. B *Chem. Rev.* **1997**, *97*, 2879. (b) Hill, C. L., Ed. *Activation and Functionalization of Alkanes*; Wiley-Interscience: New York; 1989. (c) Arndtsen, B. A.; Bergman, R. G.; Mobley, A.; Peterson, T. H. *Acc. Chem. Res.* **1995**, *28*, 154. (d) Bergman, R. G. *J. Organomet. Chem.* **1990**, *400*, 273.

(2) (a) Gupta, M.; Hagen, C.; Kaska, W. C.; Cramer, R. E.; Jensen, C. M. *J. Am. Chem. Soc.* **1997**, *119*, 840, and references therein. (b) Vigalok, A.; Kraatz, H.-B.; Konstantinovsky, L.; Milstein, D. *Chem. Eur. J.* **1997**, *3*, 253. (c) Arndtsen, B. A.; Bergman, R. G. *Science* **1995**, *270*, 1970.

10.1021/om9904450 CCC: $18.00
Publication on Web 07/20/1999

Table 1. Numbering Scheme, Yield, and Analytical Data for Complexes 2−16

complex	cmpd no.	color (yield[a], %)	anal. found (calcd) C	H	N
Cp*W(NO)(η^2-CPhCH$_2$)(Ph)	**2**	brown, (>97)	54.46 (5 76)	54.14 (5.36)	2.65 (2.42)
Cp*W(NO)(η^2-CPhCH$_2$)(*p*-tolyl)	**3p**	red-brown, (57)	54.94 (55.26)[d]	5.28 (5.38)	2.43 (2.58)
Cp*W(NO)(η^2-CPhCH$_2$)(*m*-tolyl)	**3m**	red-brown, (38)	54.94 (55.26)[d]	5.28 (5.38)	2.43 (2.58)
Cp*W(NO)(η^2-CPhCH$_2$)(CH$_2$Ph)	**4**	red, (78)	55.20 (55.26)	5.18 (5.38)	2.57 (2.58)
Cp*W(NO)(CPh=CH$_2$)(η^2-CH$_2$C$_6$H$_4$-*p*-Me)	**5**	orange, (>97)	56.16 (56.03)	5.63 (5.61)	2.60 (2.51)
Cp*W(NO)(η^2-CPhCH$_2$)(C$_6$H$_3$-*m*-Me$_2$)	**6**	red (33)	*c*		
Cp*W(NO)(CPh=CH$_2$)(η^2-CH$_2$C$_6$H$_4$-*m*-Me)	**7**	orange (66)	56.27 (56.03)	5.51 (5.61)	2.43 (2.51)
Cp*W(NO)(η^2-CPhCH$_2$)(C$_6$H$_4$-*m*,*p*-Me$_2$)	**8**	burgundy (85)	56.26 (56.03)	5.51 (5.61)	2.50 (2.51)
Cp*W(NO)(η^2-CPhCH$_2$)(η^2-CH$_2$C$_6$H$_4$-*o*-Me)	**9**	burgundy (15)	*c*		
Cp*W(NO)(η^2-CPhCH$_2$)(CH$_2$SiMe$_2$OSiMe$_3$)	**10**	mauve, (>97)	47.13 (46.98)	6.21 (6.41)	2.26 (2.28)
Cp*W(NO)(η^2-CH(η^2-Ph)CH$_2$CH(^{n}Pr)CH$_2$)	**11**	brown (57)[b]	52.18 (52.78)	6.48 (6.36)	2.60 (2.68)
Cp*W(NO)(η^2-CH(η^2-Ph)CH$_2$CH(^{n}Bu)CH$_2$)	**12**	brown (23)[b]	53.90 (53.46)	6.61 (6.57)	2.54 (2.61)
Cp*W(NO)(η^2-CH(η^2-Ph)CH$_2$CH(^{t}Bu)CH$_2$)	**13**	brown (59)[b]	*c*		
Cp*W(NO)(η^2-CH(η^2-Ph)CH$_2$CH(OEt)CH$_2$)	**14**	brown (63)[b]	50.30 (50.29)	5.91 (5.95)	2.58 (2.67)
Cp*W(NO)(η^3-*endo*-CH$_2$C(Me)C(Me)CH$_2$(η^1-CPhMe))	**15**	yellow (68)[b]	*c*		
Cp*W(NO)(CH$_2$SiMe$_3$)(η^2-CH$_2$CPh(PMe$_3$))	**16**	yellow (71)[b]	48.94 (48.78)	7.07 (6.88)	2.44 (2.28)

[a] Yield as indicated in the ^{1}H NMR spectrum of the reaction mixture unless otherwise noted. [b] Isolated yield. [c] Satisfactory analysis could not be obtained. [d] Determined as a mixture of **3m**, **3p,** and **4**.

lation of an alkane substrate to an aldehyde.[3] Maintaining reactivity at the metal center throughout the C−H bond activation process is a key concept in the development of systems capable of hydrocarbon elaboration.

In this regard, we recently described an alkane C−H bond activation process by an organotungsten complex which not only constitutes a rare example of an intermolecular alkane C−H bond activation at a tungsten metal center[4] but also represents a prototypal model of an organometallic system capable of chemically elaborating a hydrocarbon substrate. As outlined in this earlier report, the dual C−H bond activation of either *n*-pentane or *n*-hexane during the thermal decomposition of Cp*W(NO(CH$_2$SiMe$_3$)(η^2-CPhCH$_2$) (**1**) in the appropriate hydrocarbon solvent yields the novel tungstenacycles Cp*W(NO)(η^3-CHPhCH$_2$CHRCH$_2$) [R = ^{n}Pr, ^{n}Bu] regioselectively (eq 1).[4c] An inspection of their

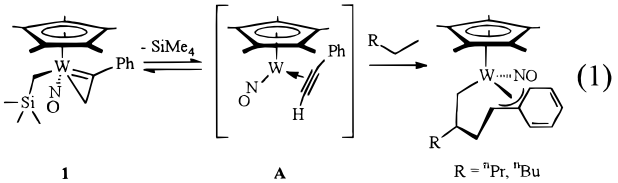

(1)

1 **A** R = ^{n}Pr, ^{n}Bu

molecular structures reveals that the incorporated hydrocarbon fragment, having lost two hydrogen atoms, has undergone a metal-mediated dehydrogenation. However, unique to this system is the chemical elaboration that extends beyond alkane dehydrogenation to encompass the coupling of the vinyl and hydrocarbyl fragments in the metal's coordination sphere.

Consistent with the proposed rate-limiting, reversible formation of acetylene complex **A** during conversions 1, it was found that the addition of excess SiMe$_4$ to the reaction mixture did indeed retard the rate of C−H activation. Additional support for the intermediacy of acetylene complex **A** is provided in our recent reports[5] of heteroatom-containing metallacycles being generated via reductive coupling reactions involving ester or nitrile substrates (e.g., eq 2).

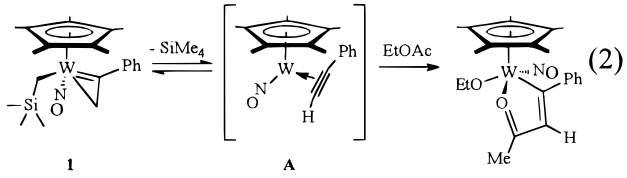

(2)

1 **A**

Since our initial report of the C−H bond activation chemistry depicted in eq 1, we have expanded the scope of our investigations to include other aliphatic and aromatic substrates. In so doing, we have discovered a quantitative single C−H bond activation process involving aryl, benzyl, and alkyl C−H bonds (eq 3), and another regioselective dual C−H activation process involving an olefinic substrate. In this paper we present the full details of this survey, including the results of kinetic, mechanistic, and competition studies.

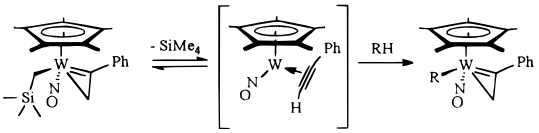

(3)

1 **A**

Results and Discussion

Analytical data and a numbering scheme for the compounds discussed in this paper are presented in Table 1. Low- and high-resolution mass spectral data (where adequate analytical data are lacking) and IR spectral data are collected in Table 2. ^{1}H and ^{13}C NMR spectroscopic data for complexes **2**−**16** are presented in Table 3, and the X-ray crystallographic data for complexes **11**, **15**, and **16** are collected in Table 4.

A. Activation of the C−H Bonds of Benzene, Methyl-Substituted Arenes, and Hexamethyldisiloxane. The activation of benzene C−H bonds is

(3) Sakakura, T.; Sodeyama, T.; Sasaki, K.; Wada, K.; Tanaka, M. *J. Am. Chem. Soc.* **1990**, *112*, 7221.

(4) (a) Waltz, K. M.; Hartwig, J. F. *Science* **1997**, *277*, 211. (b) Tran, E.; Legzdins, P. *J. Am. Chem. Soc.* **1997**, *119*, 5071. (c) Debad, J. D.; Legzdins, P.; Lumb, S. A.; Batchelor, R. J.; Einstein, F. W. B. *J. Am. Chem. Soc.* **1995**, *117*, 3288. (d) Green, M. L.; Berry, M.; Couldwell, C.; Prout, K. *Nouv. J. Chem.* **1977**, *1*, 187.

(5) (a) Legzdins, P.; Lumb, S. A. *Organometallics* **1997**, *16*, 1825. (b) Legzdins, P.; Lumb, S. A.; Young, V. G. *Organometallics* **1998**, *17*, 854.

Table 2. Mass Spectrometric and IR Spectral Data for Complexes 2−6, 8, and 10−16

cmpd no.	MS (*m*/*z*)[a]	probe temp[b] (°C)	IR (Nujol, cm^{-1})
2	529	120	1572, 1562, 1553
3p	544[c]	150	1565 (ν_{NO})[c]
3m	544[c]	150	1565 (ν_{NO})[c]
4	544	150	1591 (ν_{NO})
5	557	250	1593, 1569, 1545
6	557	250	1626 (ν_{NO})
8	557	150	1573 (ν_{NO})
10	598 [P^+ − Me] 451 [$P^+ - C_6H_{17}OSi_2$]	150	1580 (ν_{NO})
11	523	100	1571 (ν_{NO})
12	537	150	1572 (ν_{NO})
13	537.22364[d] (537.22284) [P^+] 507.22783 (507.22482) [P^+ − NO]	150	1568 (ν_{NO})
14	525	120	1560 (ν_{NO})
15	535.20809[d] (535.20715) [P^+]	120	1542 (ν_{NO})
16	615	80	1484 (ν_{NO})

[a] Values for the highest intensity parent peak of the calculated isotopic cluster (^{184}W). [b] Probe temperatures. [c] Spectrum recorded as a mixture of **3m** and **3p**. [d] High-resolution EI mass spectrum, found (calcd).

described as a representative example of the thermal activation of **1** in solution. Heating of solutions of **1** in neat benzene to 54 °C over 24 h cleanly affords the red-brown phenyl complex **2** in >97% yield (eq 4, [W] = Cp*W(NO)) as judged by ^1H NMR spectroscopic monitoring. In addition to signals attributable to the 1-metallacyclopropene fragment analogous to those in **1**, resonances in the aromatic region of the ^1H (C_6D_6) and ^{13}C ($CDCl_3$) NMR spectra of **2** are readily attributable to the phenyl ligand derived from a benzene solvent molecule.

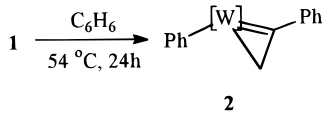

2 (4)

Thermolyses of complex **1** have been conducted in methyl-substituted arenes to assess the selectivity of acetylene complex **A** for the activation of aryl or benzylic C−H bonds. For example, thermolysis of **1** in toluene at 50 °C for 24 h affords the products depicted in eq 5 in quantitative yields.

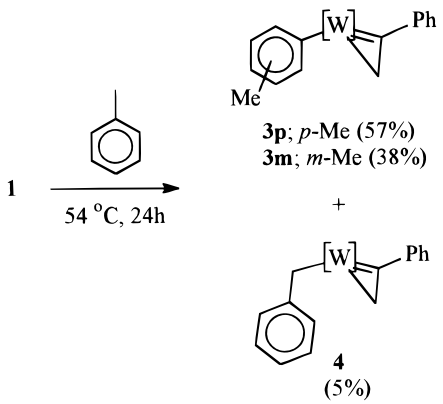

(5)

Complexes **3m** and **3p** are derived from aryl C−H bond activation of toluene by acetylene complex **A**, whereas aliphatic C−H bond activation of a benzylic C−H bond leads to the red benzyl complex **4**, albeit in very low yield. Compounds **3m** and **3p** coprecipitate, and their physical separation is hampered by their decomposition on chromatographic media. In solution, however, they are readily distinguished by utilizing ^1H COSY and NOE NMR data. Identification of benzyl compound **4** is facilitated by its alternate route of preparation employing standard metathetical protocol,[6] i.e., by treating $Cp^*W(NO)Cl_2$ with 1 equiv each of $(CH_2{=}CPh)_2Mg{\cdot}$dioxane) and $Bz_2Mg{\cdot}$(dioxane). The benzyl fragment in complex **4** is depicted as an η^1-ligand in eq 5, although the upfield chemical shift of 130 ppm attributable to C_{ipso} suggests a significant degree of η^2-character. The existence of a 1-metallacyclopropene fragment in each of these three compounds in solution is indicated by the relevant NMR signals in their ^1H and ^{13}C NMR spectra (Table 3). For example, the vinyl C_β signals in the ^{13}C NMR spectra for complexes **3p**, **3m**, and **4** appear at δ 80.3, 79.6, and 78.6, respectively, while those due to C_α occur at 234.6, 233.5, and 207.8 ppm, respectively.

The results of the thermolysis of complex **1** in *p*-, *m*-, and *o*-xylene at 54 °C are shown in Scheme 1. As in toluene, the thermolysis of **1** in these xylenes yields no products resulting from the activation of an aryl C−H bond in a position on the ring *ortho* to a methyl substituent.

The thermolysis of **1** in *p*-xylene affords the 4-methylbenzyl complex **5** that results from the activation of a methyl C−H bond. The NMR data for the η^2-benzyl and η^1-vinyl ligands in complex **5** contrast to those observed for the η^1-benzyl and cyclopropenyl ligands in benzyl complex **4**. By comparison to the same signals for complex **4**, both the downfield shift of the vinyl H signals (5.42 and 3.49 ppm) in the ^1H NMR spectrum of **5** and the shift of the vinyl C_α and C_β signals (194.7 and 115.9 ppm, respectively) into the olefinic region of the ^{13}C NMR spectrum of **5** implicate an η^1-bonding mode for the vinyl ligand. In addition, the upfield shift of the benzyl *o*-H signal (6.66 ppm) in the ^1H NMR spectrum of **5** and the high-field signal for the *ipso*-C of the benzyl ligand (115.5 ppm) in the ^{13}C NMR spectrum attest to the sp^3 character imposed on this carbon nucleus by the η^2-coordination mode of the *p*-xylyl ligand.[7] From these data it can be concluded that the 4-methylbenzyl ligand is the stronger donor in this complex, and therefore, the vinyl ligand is forced to assume the η^1-coordination mode to avoid the expansion of the tungsten valence shell to 20e.

The thermolysis of **1** in *m*-xylene under similar conditions affords aryl complex **6** and η^2-benzyl complex **7** in a 33(3):66(3) ratio. As expected, complex **6** readily decomposes on alumina I, permitting the isolation of pure **7** from their mixtures by elution with Et_2O on this solid support. Thus, ^1H NMR spectroscopic data for **6** can only be obtained from solutions of the crude mixture. The dihapto bonding of the benzyl ligand to

(6) Debad, J. D.; Legzdins, P.; Batchelor, R. J.; Einstein, F. W. B. *Organometallics* **1993**, *12*, 2094.

(7) (a) Dryden, N. H.; Legzdins, P.; Sayers, S. F.; Trotter, J.; Yee, V. C. *Can. J. Chem.* **1995**, *73*, 1035. (b) Legzdins, P.; Jones, R. H.; Phillips, E. C.; Yee, V. C.; Trotter, J.; Einstein, F. W. B. *Organometallics* **1991**, *10*, 986. (c) Dryden, N. H.; Legzdins, P.; Trotter, J.; Yee, V. C. *Organometallics* **1991**, *10*, 2857. (d) Dryden, N. H.; Legzdins, P.; Phillips, E. C.; Trotter, J.; Yee, V. C. *Organometallics* **1990**, *9*, 882.

Table 3. ^{1}H and ^{13}C NMR Spectroscopic Data for Complexes 2−16

cmpd no.	^{1}H NMR,[a] δ	^{13}C NMR,[a] δ
2	7.99 (d, $^3J_{HH}$ = 7.8 Hz, 2H, Ph−H_{ortho})	225.1 (*C*PhCH$_2$)
	7.90 (d, $^3J_{HH}$ = 7.8 Hz, 2H, Ph−H_{ortho})	179.0 (Ph−C_{ipso})
	7.27 (m, 4H, Ph−H_{meta})	143.3 (Ph−C_{ipso})
	7.18 (m, 2H, Ph−H_{para})	140.8, 130.3, 129.3, 128.9,
	4.28 (d, $^2J_{HH}$ = 6.9 Hz, J_{WH} = 6.3 Hz, 1H, CPhC*H*$_a$H$_b$)	127.5, 126.4 (Ar)
	3.71 (d, $^2J_{HH}$ = 6.9 Hz, J_{WH} = 6.3 Hz, 1H, CPhCH$_a$*H*$_b$)	110.2 (s, *C*$_5$Me$_5$)
	1.54 (s, 15H, C$_5$Me$_5$)	78.6 (CPh*C*H$_2$)
		9.6 (C$_5$*Me*$_5$)
3p	7.99 (d, $^3J_{HH}$ = 7.7 Hz, 2H, Ar−H_{ortho})	[c]234.6 (*C*PhCH$_2$)
	7.92 (d, $^3J_{HH}$ = 7.4 Hz, 2H, Ar−H_{ortho})	233.6 (*C*PhCH$_2$)
	7.27 (t, $^3J_{HH}$ = 8.1 Hz, 1H, Ar−H_{para})	178.2 (Ar−C_{ipso})
	7.14 (m, 2H, Ar−H_{meta})	175.1 (Ar−C_{ipso})
	7.01 (t, $^3J_{HH}$ = 7.4 Hz, 1H, Ar−H_{para})	144.2 (Ar−C_{ipso})
	4.30 (d, $^2J_{HH}$ = 6.6 Hz, 1H, CPhC*H*$_a$H$_b$)	139.5 (Ar−C_{ipso})
	3.76 (d, $^2J_{HH}$ = 6.6 Hz, 1H, CPhCH$_a$*H*$_b$)	142.2, 141.6, 138.4 (Ar)
	2.18 (s, 3H, Ar(*Me*))	137.9 (Ar−*C*(Me))
	1.56 (s, 15H, C$_5$Me$_5$)	
3m	7.98 (s, 1H, Ph−H_{ortho})	[c]137.2 (Ar−*C*(Me))
	7.92 (d, $^3J_{HH}$ = 7.4 Hz, 2H, Ph−H_{ortho})	130.9, 130.8, 130.4, 130.3, 130.2,
	7.78 (d, $^3J_{HH}$ = 7.3 Hz, 2H, Ph−H_{ortho})	129.9, 129.8, 129.3, 129.2, 128.8,
	7.27 (d, $^3J_{HH}$ = 8.1 Hz, 2H, Ph−H_{meta})	128.2 (Ar)
	7.14 (m, 2H, Ph)	110.9 (*C*$_5$Me$_5$)
	7.01 (t, $^3J_{HH}$ = 7.4 Hz, 1H, Ph−H_{para})	80.3 (CPh*C*H$_2$)
	4.33 (d, $^2J_{HH}$ = 6.6 Hz, 1H, CPhC*H*$_a$H$_b$)	79.6 (CPh*C*H$_2$)
	3.79 (d, $^2J_{HH}$ = 6.6 Hz, 1H, CPhCH$_a$*H*$_b$)	21.6 (Ar*Me*)
	2.25 (s, 3H, Ar(*Me*))	21.5 (Ar*Me*)
	1.56 (s, 15H, C$_5$Me$_5$)	9.9 (C$_5$*Me*$_5$)
4	7.56 (d, $^3J_{HH}$ = 7.8 Hz, 2H, Ph−H_{ortho})	207.8 (*C*Ph=CH$_2$)
	7.30 (t, $^3J_{HH}$ = 7.8 Hz, 4H, Ph−H_{meta})	149.9 (Ph−C_{ipso})
	7.11 (m, 4H, Ph−H_{meta}, −H_{ortho})	132.6 (Ph−C_{ortho})
	6.99 (t, $^3J_{HH}$ = 7.8 Hz, 1H, Ph−H_{para})	130.8 (Ph−C_{ipso})
	4.76 (s, 1H, CPh=C*H*$_a$H$_b$)	129.1, 128.8, 128.2,
	3.54 (s, 1H, CPh=C*H*$_a$H$_b$)	127.6, 126.9 (Ph)
	3.08 (d, $^2J_{HH}$ = 8.1 Hz, 1H, C*H*$_a$H$_b$Ph)	110.2 (s, C$_5$Me$_5$)
	2.60 (d, $^2J_{HH}$ = 8.1 Hz, 1H, CH$_a$*H*$_b$Ph)	78.6 (CPh=*C*H$_2$)
	1.54 (s, 15H, C$_5$Me$_5$)	9.6 (C$_5$*Me*$_5$)
5	7.39 (m, 4H, Ar−H_{ortho}, −H_{meta})	194.7 (*C*Ph=CH$_2$)
	7.10 (tt, $^3J_{HH}$ = 6.9 Hz, $^4J_{HH}$ = 1.8 Hz, Ar−H_{para})	152.6 (Ar−C_{ipso})
	6.88 (d, $^3J_{HH}$ = 7.2 Hz, 2H, Ar−H_{meta})	141.9, 134.6, 130.1,
	6.66 (d, $^3J_{HH}$ = 7.2 Hz, 2H, Ar−H_{ortho})	127.8, 127.3, 125.2 (Ar)
	5.42 (d, $^3J_{HH}$ = 0.9 Hz, 1H, CPh=C*H*$_a$H$_b$)	115.9 (CPh=*C*H$_2$)
	3.49 (d, $^3J_{HH}$ = 0.9 Hz, 1H, CPh=CH$_a$*H*$_b$)	115.5 (Ar−C_{ipso})
	3.17 (d, $^2J_{HH}$ = 6.6 Hz, 1H, C*H*$_a$H$_b$Ar)	108.8 (*C*$_5$Me$_5$)
	2.32 (d, $^2J_{HH}$ = 6.6 Hz, 1H, CH$_a$*H*$_b$Ar)	47.5 (CH$_2$Ar)
	1.91 (s, 3H, Ar(*Me*))	22.1 (Ar(*Me*))
	1.59 (s, 15H, C$_5$Me$_5$)	10.6 (C$_5$*Me*$_5$)
6	7.92 (s, 1H, Ar−H_{ortho})	233.5 (*C*PhCH$_2$)
	7.90 (s, 1H, Ar−H_{ortho})	179.8 (Ar−C_{ipso})
	7.75 (s, 1H, Ar−H_{para})	151.9 (Ar−C_{ipso})
	7.58 (d, $^3J_{HH}$ = 7.8 Hz, 2H, Ar−H_{ortho})	138.6 (Ar−*C*(Me))
	7.37 (t, $^3J_{HH}$ = 7.8 Hz, 2H, Ar−H_{meta})	137.6 (Ar−*C*(Me))
	7.17 (t, $^3J_{HH}$ = 7.9 Hz, 1H, Ar−H_{para})	134.4, 131.1, 130.2,
	4.40 (d, 1H, CPhC*H*$_a$H$_b$)	128.7 128.2 127.2 (Ar)
	3.86 (d, 1H, CPhCH$_a$*H*$_b$)	110.3 (*C*$_5$Me$_5$)
	2.38 (s, 3H, Ar(*Me*))	80.9 (CPh*C*H$_2$)
	1.61 (s, 15H, C$_5$Me$_5$)	21.6 (Ar−C(*Me*))
	1.52 (s, 3H, Ar(*Me*))	21.3 (Ar−C(*Me*))
		9.7 (C$_5$*Me*$_5$)
7	7.27 (m, 4H, Ar−H_{ortho})	208.7 (*C*Ph=CH$_2$)
	7.17 (m, 1H, Ar−H_{para})	139.8 (Ar−C_{ipso})
	7.16 (d, 1H, Ar−H_{para})	134.5, 132.3 (Ar)
	6.95 (br t, 1H, Ar−H_{meta})	131.8 (Ar−*C*(Me))
	6.79 (br d, 1H, Ar−H_{ortho})	129.9, 129.5, 129.2,
	6.70 (br s, 1H, Ar−H_{ortho})	128.3, 127.5 (Ar)
	4.88 (s, 1H, CPh=C*H*$_a$H$_b$)	110.2 (*C*$_5$Me$_5$)
	3.79 (s, 1H, CPh=CH$_a$*H*$_b$)	109.5 (Ar−C_{ipso})
	2.80 (d, $^3J_{HH}$ = 12.4 Hz, C*H*$_a$H$_b$Ar)	104.0 (CPh=*C*H$_2$)
	2.68 (d, $^3J_{HH}$ = 12.4 Hz, CH$_a$*H*$_b$Ar)	52.3 (*C*H$_2$Ar)
	2.23 (s, 3H, Ar(Me))	21.6 (Ar−C(*Me*))
	1.91 (s, 15H, C$_5$Me$_5$)	10.8 (C$_5$*Me*$_5$)

Table 3 (Continued)

cmpd no.	^{1}H NMR,[a] δ	^{13}C NMR,[a] δ
8	8.04 (s, 1H, Ar−H_{ortho}) 7.93 (d, $^3J_{HH}$ = 7.5 Hz, 2H, Ar−H_{ortho}) 7.81 (d, $^3J_{HH}$ = 7.5 Hz, 2H, Ar−H_{ortho}) 7.28 (t, $^3J_{HH}$ = 7.2 Hz, 2H, Ar−H_{meta}) 7.15 (t, $^3J_{HH}$ = 7.2 Hz, 2H, Ar−H_{para}) 7.12 (d, $^3J_{HH}$ = 7.5 Hz, 2H, Ar−H_{meta}) 4.37 (d, $^2J_{HH}$ = 6.3 Hz, 1H, CPhC$H_a$$H_b$) 3.90 (d, $^2J_{HH}$ = 6.3 Hz, 1H, CPhC$H_a$$H_b$) 2.17 (s, 3H, Ar*Me*) 2.09 (s, 3H, Ar*Me*) 1.59 (s, 15H, C_5Me_5)	232.8 (*C*PhCH$_2$) 177.8 (s, Ar−C_{ipso}) 144.2 (s, Ar−C_{ipso}) 142.5, 138.8, 138.6 (d, $^1J_{CH}$ ≈ 156 Hz, Ar) 135.7 (s, Ar−*C*(Me)) 135.2 (s, Ar−*C*(Me)) 130.1, 129.9, 129.5, (d, $^1J_{CH}$ ≈ 156 Hz, Ar) 129.1, 128.8 (d, $^1J_{CH}$ ≈ 156 Hz, Ar) 111.8 (s, *C*$_5$Me$_5$) 82.2 (dd, $^1J_{CH}$ = 152 Hz, CPh*C*H$_2$) 19.9, 19.8 (q, $^1J_{CH}$ = 126 Hz, Ar(*Me*)) 10.6 (q, $^1J_{CH}$ = 127 Hz, C$_5$*Me*$_5$)
9	6.82, 6.61, 6.40 (br, Ar) 5.31 (s, CPh=C$H_a$$H_b$) 3.77 (s, CPh=CH$_a$$H_b$) 3.10 (d, C$H_a$$H_b$Ar) 2.25 (d, CH$_a$$H_b$Ar) 2.02 (s, Ar*Me*) 1.54 (s, C_5Me_5)	[b]
10	7.93(d, $^3J_{HH}$ = 7.2 Hz, 2H, Ph−H_{ortho}) 7.29 (t, $^3J_{HH}$ = 7.2 Hz, 2H, Ph−H_{meta}) 7.13 (t, $^3J_{HH}$ = 7.5 Hz, 1H, Ph−H_{para}) 3.84 (dd, $^2J_{HH}$ = 6.0 Hz, $^5J_{HH}$ = 1.0 Hz, 1H, CPhC$H_a$$H_b$) 3.57 (dd, $^2J_{HH}$ = 6.0 Hz, $^5J_{HH}$ = 1.0 Hz, 1H, CPhCH$_a$$H_b$) 1.50 (s, 15H, C_5Me_5) 0.79 (d, $^3J_{HH}$ = 12.6 Hz, C$H_a$$H_b$SiMe$_2$OSiMe$_3$) 0.54 (s, 3H, Si*Me*$_aMe_b$OSiMe$_3$) 0.31 (d, $^3J_{HH}$ = 12.6 Hz, CH$_a$$H_b$SiMe$_2$OSiMe$_3$) 0.28 (s, 3H, SiMe$_a$*Me*$_b$OSiMe$_3$) 0.20 (s, 9H, OSiMe$_3$)	228.0 (*C*PhCH$_2$) 145.0 (Ph−C_{ipso}) 131.4, 129.7, 129.0 (Ph) 109.6 (*C*$_5$Me$_5$) 82.1 (CPh*C*H$_2$) 35.3 (*C*H$_2$SiMe$_2$OSiMe$_3$) 9.6 (C$_5$*Me*$_5$) 4.6 (*C*H$_2$Si*Me*$_a$Me$_b$OSiMe$_3$) 4.4(*C*H$_2$SiMe$_a$*Me*$_b$OSiMe$_3$) 2.5 (OSiMe$_3$)
11	6.97 (br, 2H, Ar) 6.64 (t, 1H, Ar) 2.98 (m, 1H, CH$_2$CH(^{n}Pr)CH_2CHAr) 2.51 (m, 1H, CH$_2$C*H*(^{n}Pr)CH$_2$CHAr) 1.83 (m, 1H, CH$_2$CH(^{n}Pr)CH$_2$C*H*Ar) 1.67 (m, 1H, CH_2CH(^{n}Pr)CH$_2$CHAr) 1.4−1.6 (m, 5H) 1.58 (s, 15H, C_5Me_5) 1.10 (m, 1H, CH_2CH(^{n}Pr)CH$_2$CHAr) 0.98 (t, $^3J_{HH}$ = 7.0 Hz, 3H, CH$_3$)	121.3, 121.0 (Ar) 106.5 (*C*$_5$Me$_5$) 71.3 (W*C*HAr, $^1J_{CW}$ = 15 Hz) 52.7 (WCH$_2$*C*H(^{n}Pr)) 44.2 (*C*H$_2$CH$_2$CH$_3$) 36.1 (WCH$_2$CH(^{n}Pr)), $^1J_{CW}$ = 88 Hz) 35.3 (CH$_2$CH(^{n}Pr)*C*H$_2$CHAr) 22.4 (CH$_2$*C*H$_2$CH$_3$) 15.1 (CH$_2$CH$_2$*C*H$_3$) 10.1 (C$_5$*Me*$_5$)
12	7.00 (br, 2H, ArH) 6.68 (t, $^3J_{HH}$ = 7 Hz, 1H, ArH) 3.02 (m, 2H, WCHPhCH_2CH) 2.54 (m, 1H, WCH$_2$C*H*) 1.4−1.8 (m, 6H) 1.59 (s, 15H, C_5Me_5) 1.15 (m, 2H) 1.02 (m, 1H) 0.97 (t, $^3J_{HH}$ = 7.6 Hz, 3H, CH$_3$)	122.0, 121.1 (C_{aryl}) 106.5 (*C*$_5$Me$_5$) 71.3 (W*C*HPh) 53.1 (WCH$_2$*C*H) 41.9 (CH$_3$CH$_2$CH$_2$CH$_2$) 36.3 (WCH$_2$) 34.1 (CH$_3$CH$_2$*C*H$_2$) 31.7 (CH*C*H$_2$CH) 23.9 (CH$_3$*C*H$_2$) 14.6 (CH$_3$) 10.1 (C$_5$*Me*$_5$)
13	7.17 (app t, 1H, WH$_{meta}$) 7.04 (app t, 1H, H$_{meta'}$) 6.89 (d, 1H, H$_{ortho'}$) 6.64 (d, 1H, H$_{para}$) 3.33 (d, 1H, η^2-C−H$_{ortho}$) 2.67 (m, 1H, WC$H_a$$H_b$) 1.88 (obscured, WCH$_2$C*H*(^{t}Bu)) 1.85 (br d, 1H, WCH$_2$CH(^{t}Bu)C$H_a$$H_b$) 1.78 (m 1H, WCH$_a$$H_b$) 1.31 (br dt, 1H, WCH$_2$CH(^{t}Bu)CH$_a$$H_b$) 1.10 (dd, 1H, WCH$_2$CH(^{t}Bu)CH$_2$C*H*($\eta^2$-Ph) 0.82 (s, 9H, ^{t}Bu)	136, 131, 123 (br, Ar) 121.3, 120.8 (Ar) 107.7 (*C*$_5$Me$_5$) 70.7 (W*C*HPh) 62.4 (WCH$_2$*C*H) 35.8 (*C*(CH$_3$)$_3$) 29.9 (WCH$_2$) 27.9 (C(*C*H$_3$)$_3$) 27.5 (WCH$_2$CH*(*^{t}Bu)*C*H$_2$) 10.3 (*C*$_5$Me$_5$)

Table 3 (Continued)

cmpd no.	^{1}H NMR,[a] δ	^{13}C NMR,[a] δ
14	6.95 (br, 2H, ArH)	136, 131, 123 (br, Ar)
	6.65 (t, $^3J_{HH}$ = 7 Hz, 1H, ArH)	121.25, 120.83 (Ar)
	3.99 (m, 1H, WCH)	107.72 (C_5Me_5)
	3.72 (m, 1H, OCH_2CH$_3$)	87.46 (W*C*HPh)
	3.52 (m, 1H, OCH_2CH$_3$)	68 (br)
	3.43 (m, 1H, CHCH_2CH)	64.33 (OCH_2CH$_3$)
	2.15 (m, 1H, CHCH_2CH)	58.20 (WCH$_2$*C*H)
	2.02 (m, 1H, WCH$_2$)	33.15 (WCH$_2$, $^1J_{WC}$ = 109 Hz,)
	1.54 (s, 15H, C$_5$Me$_5$)	31.36 (CH*C*H$_2$CH)
	1.35 (m, 2H, WCH$_2$C*H*)	16.02 (CH$_3$)
	1.30 (t, $^3J_{HH}$ = 8.5 Hz, 3H, OCH$_2$CH_3)	10.43 (C_5Me_5)
15	7.46 (d, $^3J_{HH}$ = 6.9 Hz, 2H, Ph−H$_{ortho}$)	157.8 (Ph−C$_{ipso}$)
	7.32 (t, $^3J_{HH}$ = 6.9 Hz, 2H, Ph−H$_{meta}$)	137.2 (η^3-*C*H$_2$C(Me)C(Me)CH$_2$CPhMe)
	7.00 (d, $^3J_{HH}$ = 6.9 Hz, 1H, Ph−H$_{para}$)	128.8 (Ph−H$_{ortho}$)
	4.04 (d, $^2J_{HH}$ = 13 Hz, 1H,	127.2 (Ph−H$_{meta}$)
	η^3-CH$_2$C(Me)C(Me)CH_aH$_b$PhMe)	121.9 (Ph−H$_{para}$)
	3.38 (d, $^2J_{HH}$ = 13 Hz, 1H,	119.5 (η^3-CH$_2$*C*(Me)C(Me)CH$_2$CPhMe)
	η^3-CH$_2$C(Me)C(Me)CH$_a$$H_b$PhMe)	113.6 (η^3-CH$_2$C(Me)*C*(Me)CH$_2$CPhMe)
	2.42 (s, 3H, η^3-CH$_2$C(Me)C(*Me*)CH$_2$PhMe)	109.3 (C_5Me$_5$)
	1.76 (s, 3H, η^3-CH$_2$C(Me)C(Me)CH$_2$Ph*Me*)	62.7 (η^3-CH$_2$C(Me)C(Me)CH$_2$*C*PhMe)
	1.52 (s, 15H, C$_5$Me$_5$)	48.5 (η^3-CH$_2$C(Me)C(Me)*C*H$_2$CPhMe)
	1.36 (s, 3H, η^3-CH$_2$C(*Me*)C(Me)CH$_2$PhMe)	33.8 (η^3-CH$_2$C(Me)C(*Me*)CH$_2$CPhMe)
	1.29 (d, $^2J_{HH}$ = 4.1 Hz, 1H,	23.3(η^3-CH$_2$C(Me)C(Me)CH$_2$CPh*Me*)
	η^3-CH$_a$$H_b$C(Me)C(Me)CH$_2$PhMe)	21.1(η^3-CH$_2$C(*Me*)C(Me)CH$_2$CPhMe)
		10.6 (C_5Me_5)
16	7.40 (m, 2H, Ph−H$_{ortho}$)	141.9 (Ph−C$_{ipso}$)
	7.11 (t, $^3J_{HH}$ = 7.5 Hz, 2H, Ph−H$_{meta}$)	131.2 (Ph−H$_{ortho}$)
	6.99 (m, 1H, Ph−H$_{para}$)	127.5 (Ph−H$_{meta}$)
	1.56 (d, $^2J_{HP}$ = 12.4 Hz, 9H, PMe$_3$)	125.4 (Ph−H$_{para}$)
	1.40 (dd, *J* = 7.8, 25 Hz, 1H, CH_aH$_b$)	106.0 (C_5Me$_5$)
	0.98 (dd, *J* = 7.8, 25 Hz, 1H, CH$_a$$H_b$)	29.4 (d, $^1J_{CP}$ = 53 Hz, W*C*Ph(PMe$_3$))
	0.88 (d, $^2J_{HH}$ = 13.5 Hz, 1H, CH_aH$_b$SiMe$_3$)	27.6 (J_{CW} = 35 Hz, *C*H$_2$SiMe$_3$)
	0.10 (s, 9H, SiMe$_3$)	11.8 ((d, $^1J_{CP}$ = 56 Hz, PMe$_3$)
	−1.24 (d, $^2J_{HH}$ = 13.5 Hz, 1H, CH$_a$$H_b$SiMe$_3$)	10.0 (C_5Me_5)
		4.6 (CH$_2$Si*Me*$_3$)
		−10.0 (d, $^2J_{CP}$ = 4 Hz, J_{CW} = 81 Hz, W*C*H$_2$CPh(PMe$_3$))

[a] ^{1}H NMR spectra recorded in C_6D_6 at RT and ^{13}C NMR spectra recorded in $CDCl_3$ at RT unless otherwise noted. [b] Spectrum not recorded. [c] ^{13}C NMR spectroscopic data for aryl compounds **3m** and **3p** are indistinguishable and are reported combined together.

Table 4. X-ray Crystallographic Data for Complexes 11, 15, and 16

	11	**15**	**16**
	Crystal Data		
empirical formula	$C_{23}H_{33}NOW$	$C_{24}H_{33}NOW$	$C_{27}H_{42}NOPSiW$
crystal habit, color	needle, yellow	block, yellow	needle, yellow
crystal size (mm)	0.19 × 0.22 × 0.42	0.50 × 0.35 × 0.25	not recorded
crystal system	monoclinic	triclinic	monoclinic
space group	C_2/c	$P1$	$P2_1/n$
volume (Å^3)	4332.3	1054.3(4)	2801.9
a (Å)[a]	19.5492(12)	8.392(2)	14.771(2)
b (Å)	17.8193(20)	9.714(4)	9.915(2)
c (Å)	13.9719(9)	13.1555(3)	19.484(2)
α (deg)	90	94.060(6)	90
β (deg)	117.112(6)	99.371(4)	100.913(8)
γ (deg)	90	91.896(4)	90
Z	8	2	4
fw (g/mol)	523.36	535.38	639.54
density (calcd) (Mg/m^3)	1.605	1.686	1.516
abs coeff (cm^{-1})	54.6	54.98	43.2
F_{000}	2071.69	532.00	1284.3
	Data Refinement		
final *R* indices[b]	R_F = 0.017, wR_F = 0.022	R_F = 0.048, wR_F = 0.047	R_F = 0.022, wR_F = 0.025
goodness-of-fit on F^2 [c]	1.05	1.58	1.31
largest diff peak and hole[d] (Å^{-1})	0.54 and −0.33	2.65 and −3.70	0.44 and −0.44

[a] Cell dimensions based on: **11**, 25 reflections, 40° ≤ 2θ ≤ 46°; **15**, 7313 reflections, 4.0° ≤ 2θ ≤ 61.2°; **16**, 25 reflections, (31° < 2θ < 40°). [b] Number of observed reflections: **11**, 2892, ($I_o > 2.5\sigma I_o$); **15**, 3798, ($I_o > 3\sigma I_o$); **16**, 3090, ($I_o > 2.5\sigma I_o$). R_F: **11**, $R_F = \sum(|F_o| - |F_c|)|/\sum|F_o|$; $wR_F = [\sum(w(|F_o| - |F_c|)^2)/\sum(wF_o)^2]^{1/2}$; **15**, $R_F = [\sum(w(|F_o|^2 - |F_c|^2)^2)]^{1/2}$; **16**, $wR_F = [\sum(w(|F_o| - |F_c|)^2)/\sum(wF_o)^2]^{1/2}$. *w*: **11**, $w = [\sigma F_o^2 + 0.0003F_o^2]^{-1}$; **15**, $w = [\sigma^2 F_o^2]^{-1}$; **16**, $w = [\sigma F_o^2 + 0.0001F_o^2]^{-1}$. [c] GOF = $[\sum(w(|F_o| - |F_c|)^2)/\text{degrees of freedom}]^{1/2}$. [d] **11**, 1.01 Å from W; **15**, near W; **16**, near W.

W in **7** is clearly apparent by comparison of its NMR spectroscopic data to those of η^2-*p*-xylyl-containing **5**.

Aryl complex **8** and η^2-benzyl compound **9** are formed in an 85(3):15(3) ratio during the thermolysis of **1** in *o*-xylene. Complex **8** is readily isolated as a red, crystalline solid from the final reaction mixture by fractional

Scheme 1

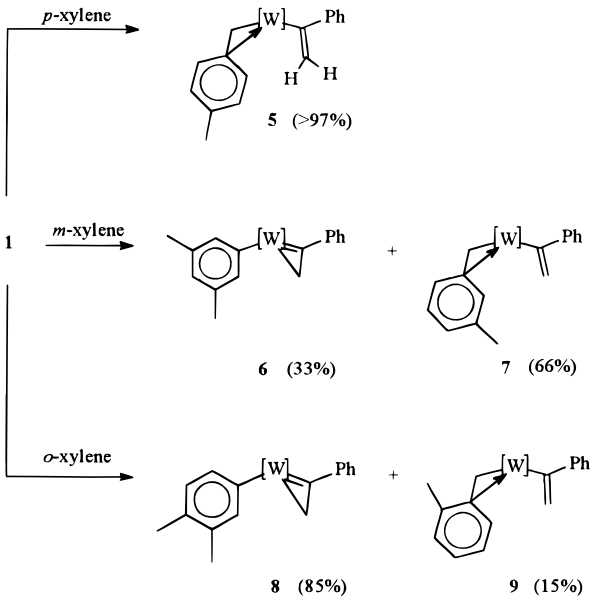

crystallization. Complex **9**, while not isolated, displays low-intensity signals in the ^{1}H and ^{13}C NMR spectra of the crude reaction mixture characteristic of an η^2-benzyl and η^1-vinyl ligand. The availability of a second aryl C−H bond in *o*-xylene relative to *m*-xylene seemingly effects a dramatic reversal in the relative proportion of products derived from aryl and benzyl C−H bond activation. This fact is discussed in more detail below.

The purple silyl ether **10** is quantitatively formed via activation of a hexamethyldisiloxane methyl C−H bond during the quantitative thermal decomposition of **1** in solution at 54 °C (eq 6). Its NMR spectroscopic features are unremarkable and analogous to those of complex **1**. This complex can be utilized as an analogue of the parent alkyl vinyl complex **1** in the kinetic study of these transformations, as described in more detail in the following section.

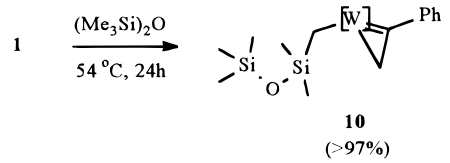

(6)

B. The Kinetics and Mechanism of Silane Elimination and C−H Bond Activation. Our kinetic investigations involve measuring the rate of conversion of **1** to the products of C−H activation in neat hydrocarbon solutions by UV−vis spectroscopy, by monitoring the change in absorbance at 350 or 360 nm. The results of these studies are collected in Table 5 and are consistent with the mechanism depicted in eq 7 (rds = rate-determining step). These conversions exhibit first-order kinetics over the entire experimental concentration range.

Table 5. Kinetic Data for the Thermal Activation of Vinyl Complexes in Hydrocarbon Solution

entry	cmpd	extruded silane or hydrocarbon	substrate	temp (K)	average k_{obs} ($\times 10^4$ s^{-1})
1	**1**	$SiMe_4$	C_6H_6	327	1.3(1)
2	**1**	$SiMe_4$	C_6D_6	327	1.3(1)
3	**1**	$SiMe_4$	*p*-xylene	314	0.12(1)
4	**1**	$SiMe_4$	*p*-xylene	320	0.48(1)
5	**1**	$SiMe_4$	*p*-xylene	327	1.1(1)
6	**1**	$SiMe_4$	*p*-xylene	340	7.8(2)
7	**1**	$SiMe_4$	*p*-xylene	348	20(1)
8	**5**	*p*-xylene	$(Me_3Si)_2O$	327	0.78(6)
9	**5-*d*$_{11}$**	*p*-xylene-d_{10}	$(Me_3Si)_2O$	327	0.17(1)

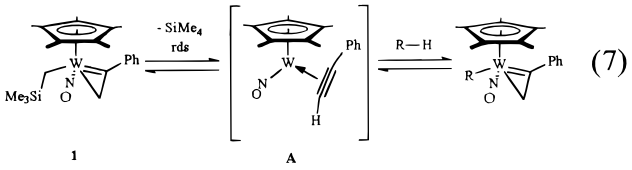

(7)

The evidence for the mechanism depicted in eq 7 is described below.

1. It has been previously reported that the addition of excess $SiMe_4$ to these reactions slows the rate of C−H activation,[8] consistent with the proposed reversible formation of acetylene complex **A**.

2. Additionally, the independence of the rate on substrate C−H activation is confirmed by monitoring the progress of the thermolysis of **1** in an equimolar mixture of C_6H_6 and C_6D_6 by ^{1}H NMR spectroscopy. Under these conditions, C−H(D) activation is indiscriminate, leading to a calculated intermolecular KIE of 1.0(1).

3. Corroborating these results, UV−vis monitoring of the thermolyses of **1** in C_6H_6 or C_6D_6 yields identical rate constants (Table entries 1 and 2, KIE = 1.0(2)).

4. Further support for the proposed rate-limiting elimination of hydrocarbon is given by the intramolecular KIE of 4.6(6) determined from the η^2-benzyl **5** → alkyl **10** and **5-*d*$_{11}$** → **10** conversions in $(Me_3Si)_2O$ (Table 5, entries 8 and 9). This relatively large intramolecular KIE establishes that the rate of reaction is dependent on vinyl C−H/C−D bond cleavage and its magnitude is comparable to others determined for such rate-limiting reductive eliminations of hydrocarbon.[9] In particular, generation of an η^2-thioaldehyde complex via β-elimination of H or D from a primary thiolate ligand in a Ti(IV) complex reported by Buchwald and Neilson affords an intramolecular KIE of 5.2 (measured at 80 °C).[9b] Samples of the deuterated analogue **5-*d*$_{11}$** are prepared by thermolyzing **1** in *p*-xylene-d_{10} for extended periods of time (>24 h) at 54 °C. This deuterated species has been characterized by ^{1}H NMR spectroscopy and mass spectrometry.

Interestingly, monitoring the thermolysis of **1** in C_6D_6 at 54 °C by ^{1}H NMR spectroscopy affords the following observations (consistent with the proposed mechanism):

1. A signal at δ 0.00 in the ^{1}H NMR spectrum is attributable to 1 equiv of $SiMe_4$ in solution.

(8) In addition to the qualitative evidence described in ref 4c in support of a rate dependence on added silane, a quantitative study of the rate dependence on [silane] in the reaction depicted in eq 2 reveals a nonlinear dependence on [silane] (i.e., saturation kinetics) according to a mechanism involving reversible, rate-limiting dissociation of silane to form **A**, followed by a faster "trapping" step involving EtOAc. Legzdins, P.; Lumb, S. A. Unpublished results. Because the second step is the microscopic reverse of the first, it follows that the C−H activation step is also reversible.

(9) (a) Caulton, K. G.; Chisholm, M. H.; Streib, W. E.; Xue, Z. *J. Am. Chem. Soc.* **1991**, *113*, 6082. (b) Buchwald, S. L.; Nielson, R. B. *J. Am. Chem. Soc.* **1988**, *110*, 3171. (c) Schrock, R. R.; Fellmann, J. D. *J. Am. Chem. Soc.* **1978**, *100*, 3359. (d) Freundlich, J. S.; Schrock, R. R.; Davis, W. M. *J. Am. Chem. Soc.* **1996**, *118*, 3643. (e) Luinstra, G. A.; Teuben, J. H. *Organometallics* **1992**, *11*, 1793.

Scheme 2

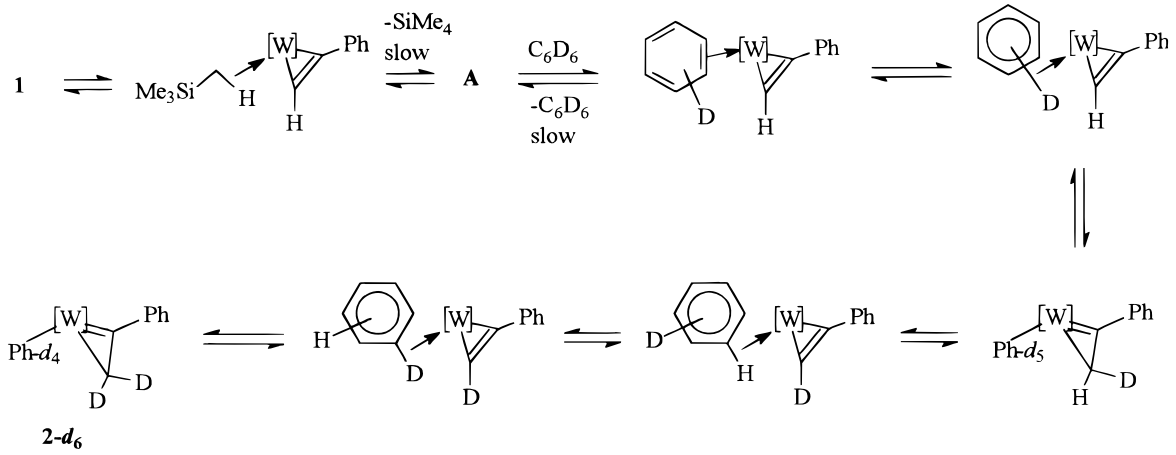

2. The metallacyclopropenyl proton resonances of **2-*d*$_7$** are absent, presumably due to the incorporation of deuterium into *both* the vinyl positions of the vinyl ligand.

The latter point is important in considering the mechanism by which silane or hydrocarbon is eliminated from the coordination sphere and by which deuterium label is introduced into the vinyl ligand in the microscopic reverse. Following the progress of the thermolysis of **1** in C_6D_6 by ^{1}H NMR reveals that the signals attributable to the vinyl protons of **1** decrease in intensity concurrently and with the same rate as **1** is being transformed. However, new resonances due to the metallacyclopropenyl protons in the product complex are not observed. The series of NMR spectra that are obtained in this way contain only those signals attributable to **1** and the product containing a *doubly deuterated* cyclopropenyl ligand. An intermediate *monodeuterated* vinyl species containing the C_6D_5 ligand (**2-*d*$_6$** in eq 8) is not observed by either ^{1}H, ^{13}C, or ^{2}H NMR spectroscopy, despite the fact that such a species is implicated in a mechanism that involves only elimination of silane or hydrocarbon in the rate-controlling step.

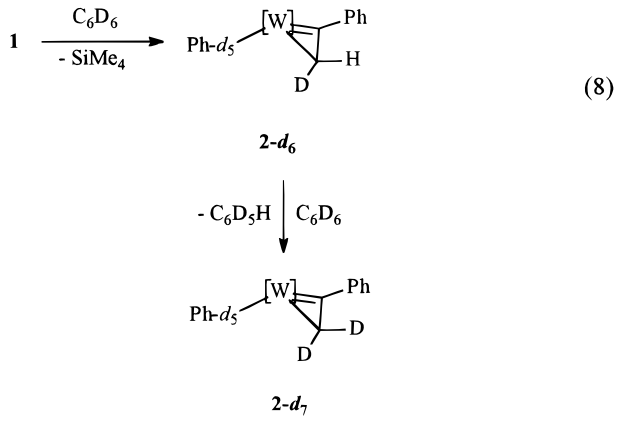

(8)

These results suggest that an equilibrium between the aryl products and π- or σ-arene complexes[10] leads to the rapid introduction of deuterium into both positions once the deuterated substrate is incorporated into the coordination sphere of tungsten (Scheme 2). Jones and co-workers describe strong evidence in support of the intermediacy of such π-arene complexes as being the source of isotopic label scrambling in their mechanistic studies of C−H activation at Rh(I) centers.[11]

Further evidence in support of the intermediacy of σ- and π-hydrocarbon complexes along the mechanistic pathway that leads to **A** is obtained by monitoring the conversion of authentic benzyl-containing **4** (vide supra) to its aryl isomers, **3p** and **3m** in toluene-d_8 by ^{1}H NMR spectroscopy at 313 K. Following a period of 60 min, approximately half of the original amount of complex **4** is converted to a mixture of complexes **3p** and **3m,** *prior* to any significant elimination of protio-toluene from or incorporation of deutero-toluene into the coordination sphere of the tungsten atom. Utilizing a half-life of 3600 s for this process, the rate constant associated with this interconversion is estimated to be ca. 1.9×10^{-4} s^{-1}. This value is more than an order in magnitude *larger* than the rate constants associated with the elimination of silane or hydrocarbon during the generation of **A** at this temperature (ca. 1.2×10^{-5} s^{-1} at 314 K).[12] These findings are inconsistent with any mechanism that involves the reversible elimination of protio-toluene from the coordination sphere of tungsten. These results suggest that the observed isomerization is being facilitated by the rapid interconversion of π- or σ-arene complexes prior to a slow elimination step.

An Eyring analysis of the kinetic data obtained for the elimination of $SiMe_4$ from **1** in *p*-xylene solution at different temperatures (Table 5, entries 3−7) yields values for the activation entropy and enthalpy which also support the rate-limiting elimination of hydrocarbon or silane to form the high-energy intermediate **A**. The moderate, positive value obtained for the activation entropy (18(3) cal (mol K)$^{-1}$) is consistent with the dissociative nature of this silane or hydrocarbon elimination step, and the magnitude of the activation enthalpy (31.0(8) kcal mol^{-1}) reflects a considerable degree of bond cleavage leading up to the highest-energy transition state.

(10) (a) Lian, T.; Bromberg, S. E.; Yang, H.; Proulx, G.; Bergman, R. G.; Harris, C. B. *J. Am. Chem. Soc.* **1996**, *118*, 3769. (b) Jones, W. D.; Hessell, E. T. *J. Am. Chem. Soc.* **1992**, *114*, 6087. (c) Bullock, R. M.; Headford, C. E. L.; Hennessy, K. M.; Kegley, S. E.; Norton, J. R. *J. Am. Chem. Soc.* **1989**, *111*, 3897. (d) Periana, R. A.; Bergman, R. G. *J. Am. Chem. Soc.* **1986**, *108*, 7332.

(11) Jones, W. D.; Feher, F. J. *J. Am. Chem. Soc.* **1986**, *108*, 4814.

(12) Bergman and Mobley have recently described the interconversion of π-complexes prior to elimination of hydrocarbon. See: Mobley, T. A.; Bergman, R. G. *J. Am. Chem. Soc.* **1998**, *120*, 3253.

Table 6. Equilibrium Constants and Free Energies for the Equilibria between C−H Activation Products Derived from Intramolecular Equilibration

equilibrium	K_{eq}	K_{eq} (per C−H bond)	$\Delta G°_{327K}$ (per C−H bond, kcal mol^{-1})
aryl **3m** ⇌ aryl **3p**[a]	1.5(2)	3.0(4)	−0.7(1)
aryl [**3m** + **3p**] ⇌ benzyl **4**	0.05(2)	0.05(2)	1.9(2)
aryl **6** ⇌ benzyl **7**	0.18(4)	0.06(1)	1.8(1)
aryl **8** ⇌ benzyl **9**	2.0(2)	0.33(4)	0.7(1)

[a] The yield of **4** is assumed to be minimal.

C. Selectivity in the Activation of Arene, Benzyl, and Siloxyl C−H Bonds. Intramolecular C−H Bond Selectivity. The intramolecular C−H bond selectivity exhibited by **A** in the presence of methyl-substituted arenes is considered first. As noted above, no products of *ortho*-C−H bond activation are observed in any of the cases studied. This selectivity is typical of such activation processes[13,14] and presumably arises as a result of the steric shielding of the *ortho*-C−H bonds by the methyl substituent in each case.

Mixtures of aryl and benzyl products at equilibrium are obtained during the thermolytic activation of **1** in toluene, and *o*- and *m*- xylene, as a result of the interconversion of σ- or π-arene complexes (Scheme 2). The associated equilibrium constants for these distributions are derived from the ratios of products. A "per C−H bond" ratio and equilibrium constant are calculated by correcting the amount of each product for the number of symmetry-equivalent substrate C−H bonds that lead to its formation. Once in hand, the equilibrium constants permit the estimation of the associated free energies of these equilibria.[15] The pertinent data are collected in Table 6.

That aryl C−H bond activation is favored in these equilibria (as evinced by the preponderance of aryl C−H bond activation products) is not surprising, given that Bergman et al. have shown that the stronger C−H bond gives rise to the stronger M−C bond upon C−H bond cleavage.[16] According to the Bryndza−Bercaw relationship,[17] the stronger C−H bond is preferentially cleaved, and this indicates that the difference in the W−C bond strengths is greater than that of the conjugate C−H bond strengths.

A noteworthy general trend in these conversions is the increased proportion of benzylic C−H bond activation that is observed as the methyl substituents in these xylenes become further separated in space, thereby shielding a greater number of arene C−H bonds. The relative amount of benzyl C−H activation follows the trend: *p*-xylene > *m*-xylene > *o*-xylene ≈ toluene. It is only when three of the four arene C−H bonds in *m*-xylene are blocked to activation by **A** by the methyl substituents that the activation of the benzyl C−H bonds becomes competitive with aryl C−H bond activation. Even in this case, the greater proportion of benzyl C−H activation remains a statistical effect, due to the number of symmetry-equivalent benzyl C−H bonds. An analysis of the energetics of these equilibria on a "per C−H bond" basis reveals that aryl C−H activation remains the energetically favorable process in all cases.

Table 7. Approximate Equilibrium Free Energies for Mixtures of Various Vinyl Complexes

equilibrium	K_{eq}	K_{eq} (per C−H bond)	$\Delta G°_{327K}$ (per C−H bond, kcal mol^{-1})
p-xylyl **5** ⇌ phenyl **2**	1.4(1)	1.4(1)	−0.2(1)
p-xylyl **5** ⇌ alkyl **10**	1.4(1)	0.5(1)	0.5(1)
phenyl **2** ⇌ alkyl **10**	1.1(1)	0.4(1)	0.6(1)

Intermolecular Competition Experiments. Competition studies employed to assess the intermolecular kinetic selectivity of **A** for *p*-xylene, hexamethyldisiloxane, and benzene C−H bonds also reveal some interesting trends. The normalized rate ratios for these competition experiments have been determined by quantifying the proportion of C−H activation products that result from the generation of **A** irreversibly in 1:1 (mol:mol) combinations of benzene, *p*-xylene, and hexamethyldisiloxane solvents. The thermal equilibration of the product distributions at early reactions times (at approximately 20% conversion) is presumed to be minimal. and therefore the ratios of products will reflect a kinetic selectivity by **A**. The resulting relative kinetic selectivity scale for C−H bond activation (on a per-C−H-bond basis) in this series of substrates takes the order sp^2 > sp^3-benzyl > sp^3-alkyl. The "per-C−H-bond" normalized rate ratio (which can be viewed as a probability scale) is calculated to be 1:0.7:0.3 for sp^2-aryl:sp^3-benzyl:sp^3-alkyl C−H bonds. The clear preference for the activation of benzyl C−H bonds over silane C−H bonds in these competition experiments is surprising. However, significant π-arene interactions between aromatic substrate and **A** during the initial complexation event presumably increase the probability of arene and benzyl C−H bond activation with respect to paraffinic C−H bond activation. In addition, steric influences probably also contribute to the kinetic selectivity by **A** for different classes of C−H bonds,[18] and the observed preference for activation of the benzyl C−H bond over the alkyl C−H bond in hexamethyldisiloxane might arise as a result of the smaller steric profile for *p*-xylene.

Thermal equilibration of these mixtures is accomplished by heating them at 327 K over a period of 96 h. The resulting distributions of products reflect the relative stability of the complexes (Table 7). Correction of $\Delta G°$(327 K) for the entropic contribution made by the number of equivalent C−H bonds in each substrate affords $\Delta G°_{corr}$(327 K), the value of which reflects the equilibrium preference on a "per-C−H-bond" basis.

The stability of the complexes, which are largely influenced by the M−C bond strengths as described above, follow the expected trend of the conjugate C−H bond strengths. Thus, the stability trend for the hydrocarbyl vinyl complexes takes the form Ph > alkyl ≈ benzyl.[13] It is interesting that the *p*-xylene benzyl C−H bond is preferred over the silane C−H bond. However,

(13) Bennett, J. L.; Wolczanski, P. T. *J. Am. Chem. Soc.* **1997**, *119*, 10696.
(14) Burger, P.; Bergman, R. G. *J. Am. Chem. Soc.* **1993**, *115*, 10462.
(15) While Van't Hoff analyses yield more accurate free energy determinations, the thermal instability of the aryl vinyl complexes at elevated temperatures (>60 °C) over the duration of the experiment obviates such an analysis.
(16) Buchanan, J. M.; Stryker, J. F.; Bergman, R. G. *J. Am. Chem. Soc.* **1986**, *108*, 1537.
(17) Bryndza, H. E.; Fong, L. K.; Paciello, R. A.; Tam, W.; Bercaw, J. E. *J. Am. Chem. Soc.* **1987**, *109*, 1444.
(18) Janowicz, A. H.; Bergman, R. G. *J. Am. Chem. Soc.* **1983**, *105*, 3929.

Scheme 3

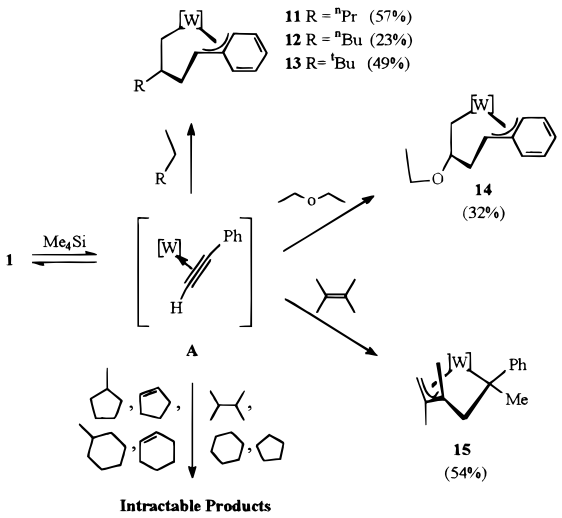

in measuring these thermodynamic equilibria one must keep in mind that the hapticity of the vinyl ligand is a variable which presumably contributes to the stability of these complexes. In other words, the balance of the C−H and M−C bond strengths is not the sole influence on the position of these equilibria, and the fact that the *p*-xylyl ligand is capable of binding to tungsten in an η^2 fashion is a stabilizing effect that presumably influences the position of the equilibrium in the last case.

D. Dual C−H Bond Activation in Aliphatic Hydrocarbons. Since our initial report of the double C−H activation of *n*-pentane and *n*-hexane by **1** under thermolysis conditions,[4c] thermolyses of **1** in the presence of a variety of other hydrocarbons have been performed in an attempt to determine the scope and limitations of this activation process. The results of these investigations are summarized in Scheme 3.

Thermolysis of **1** in the presence of *n*-pentane, *n*-hexane, 2,2-dimethylbutane, and diethyl ether results in their double C−H bond activation, affording the η^3-benzylmetallacycles **11**, **12**, **13**, and **14,** respectively. The complexes are isolated in moderate yields as yellow or yellow-brown crystals, the ^{1}H NMR spectra of the reaction mixtures revealing that the crude yields fall in the range 50−70%. These complexes are moderately air-stable in the solid state, persisting for up to 24 h in air with little measurable decomposition.

Characterization of these metallacycles is facilitated by the solid-state molecular structure of **11** (Figure 1), which has been established by an X-ray crystallographic analysis. Clearly, a molecule of pentane has been incorporated into the coordination sphere of the tungsten atom via two C−H bond cleavage processes, i.e., one at the terminal position binding the molecule to the metal, and the second in the β-position facilitating its fusion to the cyclopropenyl ligand. Single M−C and C−C[19] bonding contacts in the W−C(19) and C(19)−C(20) links (2.301(5) and 1.510(5) Å, respectively) implicate that the 1-metallacyclopropene fragment has been hydrogenated to yield the saturated W−CHPh−CH$_2$ fragment. The hydrocarbyl fragments are fused by a single bond of distance 1.535(7) Å between C(7) and C(20). These metallacycles are stabilized as 18e species by virtue of a W-η^3-benzyl interaction, as evinced by the W contacts at C(19), C(21), and C(22) of 2.301(4), 2.381(1), and 2.371(4) Å, respectively. The structural parameters for this η^3-benzyl interaction are similar to those found in other structurally characterized η^3-benzyl complexes.[20]

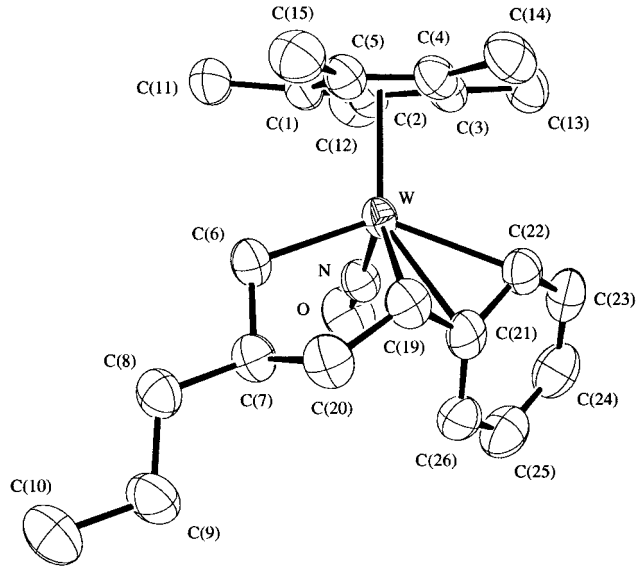

Figure 1. ORTEP plot of the solid-state molecular structure of complex **11** depicting 50% probability ellipsoids. Selected interatomic distances (Å) and angles (deg): W−N = 1.767(4), W−Cp* = 2.051, W−C(6) = 2.226(3), W−C(19) = 2.301(5), W−C(21) = 2.381(4), W−C(22) = 2.371(4), N−O = 1.225(6), C(6)−C(7) = 1.524(6), C(7)−C(20) = 1.535(7), C(19)−C(20) = 1.510(5), C(19)−C(21) = 1.419(5), C(23)−C(24) = 1.349(7), C(21)−C(22) = 1.432(5), C(24)−C(25) = 1.412(6), C(21)−C(26) = 1.440(6), C(25)−C(26) = 1.346(6), C(22)−C(23) = 1.421(6), N−W−C(6) = 88.02(15), C(6)−W−Cp* = 108.35, N−W−C(19) = 111.51(15), N−W−C(21) = 88.19(16), N−W−C(22) = 93.34(16), C(19)−W−Cp* = 124.72, N−W−Cp* = 123.76, C(6)−W−C(19) = 71.82(16), C(21)−W−Cp* = 139.03, C(6)−W−C(21) = 96.51(13), C(22)−W−Cp* = 110.82, C(6)−W-C(22) = 131.34(15), W−N−O = 174.3(3).

The broadness or complete lack of ^{1}H and ^{13}C NMR signals attributable to the ^{1}H and ^{13}C nuclei involved in the η^3-benzyl interaction in the room-temperature NMR spectra of complexes **11**−**14** is remarkable. It has been demonstrated previously that complexes of this type can undergo a rapid η^3-η^1-η^3 interconversion (shown below) that equilibrates the *ortho*/*ortho*′ and *meta*/*meta*′ H and C magnetic environments.[20,21]

The VT behavior of *tert*-butyl complex **13** has been examined in detail. At 313 K, the ^{1}H NMR spectrum (CD_2Cl_2) of complex **13** displays broadened downfield signals attributable to the protons in the phenyl ring. Broad triplets at 7.10 and 6.70 ppm integrating for 2 H and 1 H are tentatively assigned to the *meta*- and *para*-H protons, respectively. Signals attributable to the

(19) Pauling, L. *The Nature of the Chemical Bond*, 3rd ed.; Cornell University Press: Ithaca, New York, 1960; Chapter 7.

(20) (a) Carmona, E.; Marin, J. M.; Paneque, M.; Poveda, M. L. *Organometallics* **1987**, *6*, 1757. (b) Bleeke, J. R.; Burch, R. R.; Coulman, C. L.; Schardt, B. C. *Inorg. Chem.* **1981**, *20*, 1316. (c) Burch, R. R.; Muetterties, E. L.; Day, V. W. *Organometallics* **1982**, *1*, 188.

(21) (a) Cotton, F. A.; Marks, T. J. *J. Am. Chem. Soc.* **1969**, *91*, 1339. (b) Cotton, F. A.; LaPrade, M. D. *J. Am. Chem. Soc.* **1968**, *90*, 5418.

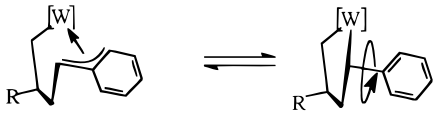

[W] = Cp*W(NO)

ortho protons are distinctly absent at this temperature. Cooling of the sample results in the collapse of the triplet at 7.10 ppm to a pair of doublets and the triplet at 6.70 to a set of doublets of doublets, while doublets of doublets centered around 6.90 and 3.43 ppm become apparent and intensify upon lowering the temperature. Fine structure is evident in all five signals at 253 K, and no further change occurs in the spectrum upon cooling to 233 K. The rate of this fluxional process at the coalescence temperature may be determined utilizing the separation of the H_m and $H_{m'}$ signals in the ^1H NMR spectrum recorded at 233 K. The 67(1) Hz separation of these two signals corresponds to a rate of rotation of 149(2) Hz at coalescence ($T = 290$ K).[22] The activation energy for this process at this temperature is therefore 14.1(1) kcal mol^{-1}.

E. Selectivity in the Dual C−H Activation of Saturated Hydrocarbons. In discussing the microscopic nature of the selectivity that yields the η^3-benzylmetallacycles **11**−**14**, the proposed mechanism by which they are formed must be considered (Scheme 4).[4c] Numerous attempts have been made to prepare the proposed intermediate species by alternative synthetic methods in an attempt establish their existence along the reaction pathway. None were successful. Regardless, ample literature precedents exist to support the mechanism depicted in Scheme 4 and the individual transformations that comprise it.[23]

The selectivity exhibited by **A** toward activation of particular alkane C−H bonds has been assessed by conducting these thermolyses in the presence of a variety of aliphatic substrates. It is worth noting that all the products of dual C−H bond activation arise from the activation of C−H bonds at the terminal and β-positions in a hydrocarbon chain, leading to the conclusion that a selectivity for terminal C−H bonds exists in this reaction. However, as indicated in Scheme 3, the thermolyses of complex **1** in cyclopentane, cyclopentene, cyclohexane, and cyclohexene each lead to the formation of a plethora of unidentifiable products, as evinced by the number of Cp* methyl resonances in the ^1H NMR spectra of the resulting reaction mixtures. This suggests that a terminal methyl substituent is necessary for the clean conversion of **1** to tractable products. The formation of the 18e metallacyclic products appears to be sensitive to the substitution at the β-C nucleus proximal to the terminal site of C−H activation as well. For example, only an oily tar is obtained from the thermal activation of **1** in 2,3-dimethylbutane, yet complex **13** is generated in good yields during the thermolysis of **1** in 2,2-dimethylbutane.

Scheme 4

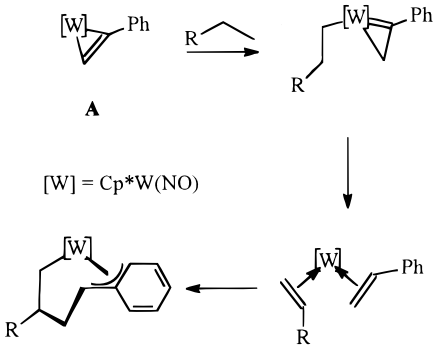

The selectivity exhibited in these reactions is proposed to arise as a result of steric interactions that come into play during the formation and subsequent isomerization of bis(olefin) complex **C** (shown below, with the NO ligand eclipsed by W) and is not regarded as a manifestation of an ability or inability by **A** to activate particular C−H bonds.

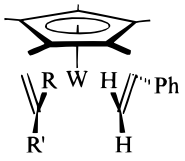

C

Thus, the dehydrogenation of an alkane containing a terminal ethyl substituent affords an α-olefin CH_2=CHR (R = H) to which the η^2-CHPh=CH_2 ligand cleanly couples in **C**. On the other hand, branched or cyclic aliphatic substrates yield multisubstituted, internal olefins upon dehydrogenation (R, R′ ≠ H). In these cases, unfavorable steric interactions between the substituents of the internal olefin and the other ligands in the W coordination sphere lead to the decomposition of **C**, presumably by promoting olefin dissociation or by slowing the rate of coupling so that decomposition pathways become kinetically competitive. The regioselectivity extant in the formation of metallacycles **11**−**14** is also worth noting. The 3,5-substitution in the metallacycle ring is typical of such metal-mediated couplings of asymmetric olefins or acetylenes.[24]

F. Dual C−H Bond Activation in an Olefinic Substrate. The thermolysis of complex **1** at 54 °C for 24 h in 2,3-dimethyl-2-butene, a hydrocarbon substrate lacking β-hydrogens, leads to an alternate mode of reactivity. In this instance, moderate yields of yellow, crystalline *endo*-allyl complex **15** are obtained (eq 9). Fusion of the olefinic fragment to the vinyl fragment has occurred in a manner reminiscent of the formation of compounds **11**−**14**, although fusion occurs at the α-C of the vinyl fragment and the two C−H bond activations in this case occur at the trans-γ positions in the olefinic substrate.

The solid-state molecular structure of **15** has been established by an X-ray crystallographic analysis and

(22) Utilizing NMR spectroscopy, the rate of a chemical exchange process at the coalescence temperature of the exchanging magnetic environments is given by the equation $k = \pi\Delta\nu/2^{1/2}$, where $\Delta\nu$ (Hz) is the frequency separation of the two signals at the low-temperature exchange limit. For more details, see: Günther, H. *NMR Spectroscopy*; Wiley: New York, 1980.

(23) See, for example: (a) McDade, C.; Bercaw, J. E. *J. Organomet. Chem.* **1985**, *279*, 281. (b) Doherty, N. M.; McDade, C.; Bercaw, J. E. In *Organometallic Compounds. Synthesis, Structure, and Reactivity, Vol. 1*; Shapiro, B. L., Ed.; Texas A & M University Press: College Station, TX, 1983.

(24) (a) Hill, J. E.; Balaich, G.; Fanwick, P. E.; Rothwell, I. P. *Organometallics* **1993**, *12*, 2911.

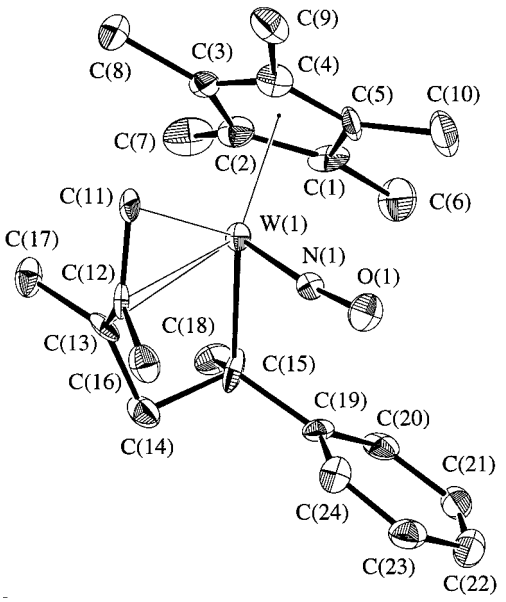

Figure 2. Solid-state molecular structure of **15** with 50% probability thermal ellipsoids being shown. Selected interatomic distances (Å) and angles (deg): W(1)−N(1) = 1.748(5), N(1)−O(1) = 1.230(7), W(1)−C(15) = 2.353(9), W(1)−C(11) = 2.249(7), W(1)−C(12) = 2.331(7), W(1)−C(13) = 2.353(7), C(15)−C(18) = 1.535(10), C(12)−C(13) = 1.397(10), C(11)−C(12) = 1.425(11), C(13)−C(14) = 1.493(12), C(14)−C(15) = 1.593(11), W(1)−N(1)−O(1) = 173.5(6), W(1)−C(15)−C(14) = 96.5(5), W(1)−C(15)−C(19) = 113.1(5), C(15)−C(14)−C(13) = 99.0(7), C(12)−C(13)−C(14) = 122.4(7), C(13)−W(1)−C(15) = 59.9(3), C(17)−C(13)−C(12)−C(16) = 143.0(7), C(11)−C(12)−C(13)−C(14) = 144.9(7).

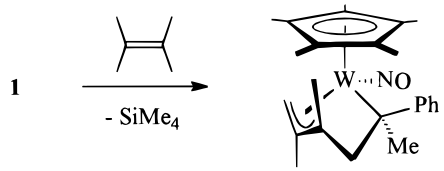

(9)

15

is illustrated in Figure 2. The allylic W−C(11), W−C(12), and W−C(13) bond lengths of 2.249(7), 2.331(7), and 2.353(7) Å, as well as the respective C(11)−C(12) and C(12)−C(13) contacts of 1.425(11) and 1.397(10) Å, are nearly identical to those present in similar structurally characterized allyl nitrosyl complexes of tungsten.[25] The C(15)−C(18) bond distance of 1.535(10) Å implies that saturation of the vinyl fragment has occurred, and the W−C(15) distance of 2.353(7) Å is indicative of a long W−C single bond. Of note is the acute C(13)−C(14)−C(15) angle of 99.0(7)° in the constrained pseudo-four-membered ring that results from the fusion of the two hydrocarbyl fragments.

The case of the dual C−H activation of 2,3-dimethyl-2-butene is unique in that, in the absence of accessible β-C−H bonds, an entirely different mode of reactivity results (Scheme 5). As in the examples described above, the activation of a methyl C−H bond presumably affords an intermediate η^3-allyl, η^1-vinyl complex (**D**).[26] For reasons of clarity, the allyl α-C in **D** has been highlighted as a point of reference. At this stage it is proposed that the allyl and vinyl ligands couple to yield a diene complex (**E**) in a process similar to that recently reported by Ipaktschi and co-workers for a CpW(NO) allyl/acetylide-containing complex.[25a] Activation of a *trans*-methyl C−H bond in the resultant diene ligand yields an allyl olefin hydride intermediate (**F**), and transfer of the hydride to the olefin affords complex **15**. A point regarding the formation of complex **15** is worth mentioning. Only the least-substituted allyl fragment is formed in the final product. While the second C−H bond activation that affords the allyl function *could* occur at the endocyclic position (*) in **F** (as observed in the CpW(NO)-based system reported by Ipaktschi and co-workers[25a]), the internal-allyl-containing complex is not observed as a byproduct. The constrained geometry of the metallacyclic fragment and the considerable ring strain that must be overcome to cleave one of the endocyclic methylene C−H bonds at the W center probably render this pathway energetically inaccessible.

Scheme 5

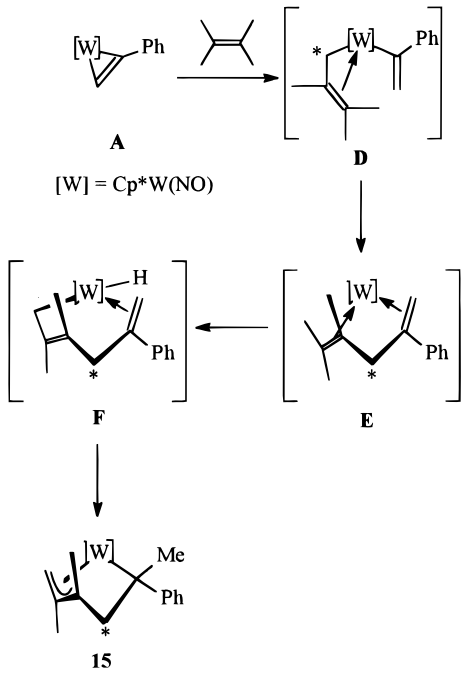

G. Attempted Trapping of Cp*W(NO)(η^2-PhC≡CH) (A) with PMe_3. We have previously reported the trapping of **A** in coupling reactions between the acetylene ligand and ester or nitrile substrates (e.g., eq 2).[5] An alternative means of trapping such transient acetylene complexes involves their coordination by Lewis bases (such as phosphines) that do not react with the acetylene ligand.[27] Our efforts to trap thermally generated **A** in this manner employing PMe_3 at 54 °C result instead in attack by the nucleophilic phosphine at the Ph-substituted α-C of the cyclopropenyl ligand, affording the zwitterionic metallacyclopropane complex **16** (eq 10, ([W] = Cp*W(NO)).

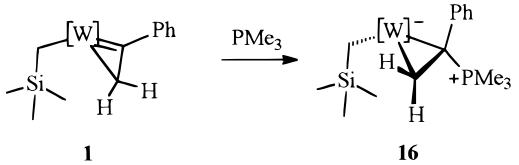

(10)

1 **16**

(25) (a) Ipaktschi, J.; Mirzaei, F.; Demuth-Eberle, G. J.; Beck, J.; Serafin, M. *Organometallics* **1997**, *16*, 3965. (b) Greenhough, T. J.; Legzdins, P.; Martin, D. T.; Trotter, J. *Inorg. Chem.* **1979**, *18*, 3268.

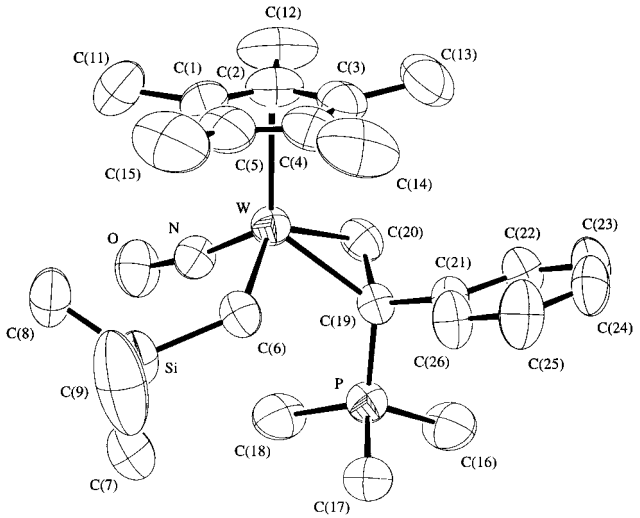

Figure 3. Solid-state molecular structure of complex **16** with 50% probablility ellipsoids. Selected interatomic distances (Å) and angles (deg) [C = C(19)−C(20) midpoint]: W−N = 1.748(4), N−O = 1.255(4), W−C(19) = 2.243(4), W−C(20) = 2.155(5), W−C(6) = 2.258(4), C(19)−C(20) = 1.463(7), C(19)−P = 1.768(4), C(19)−C(21) = 1.515(6), W−C = 2.074, W−N−O = 170.9(3), C(6)−W−C(19) = 88.5-(2), C(6)−W−C(20) = 126.7(2), N−W−C(20) = 91.9(2), N−W−C(19) = 103.7(2), C(19)−W−C(20) = 38.8(3), W−C(20)−C(19) = 73.9(3), W−C(19)−C(20) = 67.3(3).

This conversion proceeds rapidly and cleanly at room temperature, indicating that nucleophilic attack by phosphine occurs prior to H-elimination from the vinyl ligand. A view of the solid-state molecular structure of **16** is presented in Figure 3. Solution ^{1}H, ^{13}C, and ^{31}P NMR spectroscopic data indicate that the solid-state structure of **16** is maintained in solution. For instance, the downfield resonance of the P nucleus (34 ppm) attests to its phosphonium character, and coupling of the P signal to the metallacycle carbon nuclei ($^{1}J_{CP}$ = 53 Hz, $^{2}J_{CP}$ = 4 Hz) indicates that the integrity of the metallacyclopropane ring is maintained in solution.

Attempts to trap **A** in the presence of larger phosphines such as $PPhMe_2$ and PPh_2Me (room temperature, NMR scale) afford complexes analogous to **16**. Utilizing pyridine or *tert*-butyl isocyanide as potential trapping agents affords either products of C−H bond activation or products of ^{t}BuNC insertion into the W−C bonds of **1**, respectively.

Conclusions

C−H bond activation effected by acetylene complexes is a rare phenomenon.[28] The activation of C−H bonds in a wide range of hydrocarbon substrates has been demonstrated to occur following the thermal activation of Cp*W(NO)(CH_2SiMe_3)(η^2-CPhCH_2) (**1**) to the acetylene complex Cp*W(NO(η^2-PhC≡CH) (**A**). In cases where only one C−H bond is activated, the conversions are clean and quantitative. Thus, the activation of a benzene C−H bond yields the corresponding phenyl complex. In the case of methyl-substituted arenes, mixtures of aryl and benzyl complexes are obtained. In these reactions, no products of *ortho*-C−H bond activation are observed, due to the steric shielding of the *ortho*-C−H bond by the methyl substituent.

The mechanisms by which RH is eliminated from Cp*W(NO)(R)(CPhCH_2) and hydrocarbon C−H bond activation is accomplished in the resultant acetylene complex **A** have been investigated. Kinetic and mechanistic studies are consistent with a rate-limiting, reversible silane or hydrocarbon elimination step that affords acetylene-containing **A**. Hydrocarbon C−H bond activation "traps" **A** in a faster reversible step, affording the observed hydrocarbyl products. Rapid scrambling of deuterium label into the vinyl positions and the rapid appearance of equilibrium mixtures of aryl C−H bond activation products at short reaction times are consistent with the transiency of hydrocarbon σ- and π-complexes prior to both the rate-limiting elimination of hydrocarbon to afford **A** and the activation of a substrate C−H bond by **A** in the microscopic reverse.

The proportion of aryl and benzyl C−H bond activation is dependent upon the relative number of accessible aryl and benzyl C−H bonds. Intramolecular competition studies reveal that, statistically, the stronger C−H bond is preferentially activated and gives rise to the greater proportion of product. This feature is also manifested in the thermodynamic intermolecular C−H bond selectivity exhibited by **A**. The observed trends follow those reported previously, with the stronger C−H bond being the preferred site of activation, and are consistent with the proposed mechanism of C−H activation.

The dual C−H bond activation of aliphatic hydrocarbons represents a unique case in which the dehydrogenation of a hydrocarbon molecule is facilitated by the vinyl ligand functioning as an intramolecular hydrogen acceptor. In these conversions, tractable products are only obtained in the presence of aliphatic substrates which contain an ethyl substituent. This selectivity is presumed to result from steric constraints within the bis(olefin) reductive coupling step. The dual C−H activation of 2,3-dimethyl-2-butene represents a unique case in which the absence of β-hydrogens in the hydrocarbyl fragment enforces an alternate mode of reactivity.

There are two key factors to the viability of this dual C−H activation process. The first is the ability of **A** to activate hydrocarbon C−H bonds, and the second is the ability of both the acetylene ligand in **A** and the vinyl ligand that is generated in the C−H activation event to function as hydrogen acceptors. It remains to gener-

(26) It is presumed that the allyl ligand is the stronger donor ligand of the two, forcing the vinyl ligand to assume an η^1-bonding interaction with the tungsten center to avoid an expansion of the valence shell to 20e.

(27) (a) Vollhardt, K. P. C. *Acc. Chem. Res.* **1977**, *10*, 1. (b) Buchwald, S. L.; Nielsen, R. B. *Chem. Rev.* **1988**, *88*, 1047. (c) Broene, R. D.; Buchwald, S. L. *Science* **1993**, *261*, 1696. (d) Negishi, E.-I.; Takahashi, T. *Acc. Chem. Res.* **1994**, *27*, 124. (e) Casey, C. P.; Carino, R. S.; Hayashi, R. K.; Schladetzky, K. D. *J. Am. Chem. Soc.* **1996**, *118*, 1617. (f) Wong, K. L. T.; Thomas, J. L.; Brintzinger, H. H. *J. Am. Chem. Soc.* **1974**, *96*, 3694. (g) Rosenthal, U.; Ohff, A.; Michalik, M.; Görls, H.; Burlakov, V. V.; Shur, V. B. *Angew. Chem., Int. Ed. Engl.* **1993**, *32*, 1193.

(28) (a) The hydromethylation of acetylene to propylene has been observed for complexes of iron, nickel, and platinum in the presence of methane, although the mechanism of this conversion is unknown and the homogeneity of these reactions is purported to be suspect. See: Shilov, A. E. In *Activation and Functionalization of Alkanes*; Hill, C. L., Ed.; John Wiley & Sons: New York, 1989; Chapter 1. (b) A zirconocene acetylene complex has been reported to activate the C−H bonds of the Cp ligand. See: Rosenthal, U.; Ohff, A.; Michalik, M.; Görls, H.; Burlakov, V. V.; Shur, V. B. *Angew. Chem,. Int. Ed. Engl.* **1993**, *32*, 1193. (c) A zirconocene benzyne complex has been reported to activate benzene C−H bonds. See: Erker, G. *J. Organomet. Chem.* **1977**, *134*, 189.

alize this chemistry so as to introduce functionality into the vinyl ligand.

Experimental Section

General Methods. All reactions and subsequent manipulations were performed under anaerobic and anhydrous conditions under either high vacuum or an atmosphere of dinitrogen or argon. General procedures routinely employed in these laboratories have been described in detail previously.[29] The organometallic reagent, Cp*W(NO)(η^2-CPhCH$_2$)(CH$_2$SiMe$_3$) (**1**), was prepared according to the reported procedure.[4c] Benzene, toluene, *o*-, *m*-, and *p*-xylene, hexane, pentane, diethyl ether, 2,2-dimethylbutane, 2,3-dimethylbutane, 2,3-dimethylbutene, cylcohexane, methylcyclohexane, cyclopentane, cyclopentene, and hexamethyldisiloxane (Aldrich) were distilled or vacuum transferred from sodium or sodium/benzophenone ketyl. Benzene-d_6, tetramethylsilane-d_{12}, and *p*-xylene-d_{10} were vacuum transferred from sodium or sodium/benzophenone ketyl. Where appropriate, ^{1}H homonuclear decoupling experiments, GRADCOSY, NOE, HMQC, HMBC, VT ^{1}H and^{13}C experiments, and gate-decoupled ^{13}C NMR experiments were performed to facilitate ^{1}H and ^{13}C spectral assignments.

X-ray Diffraction Studies. Data collection and structure solution for complex **15** was conducted at the University of British Columbia. All measurements were recorded on a Rigaku/ADSC CCD area detector with graphite-monochromated Mo Kα radiation. The data were collected at −93(1) °C to a maximum 2θ value of 61.2°. Data were collected in 0.50 oscillations with 45.0 s exposures. A sweep of data was collected using ϕ oscillations from 0.0° to 190.0° at $\chi = -90°$, and a second sweep was performed using ω oscillations between −23.0° and 18.0°. The crystal-to-detector distance was 39.20(2) mm. The detector swing angle was −10.0°. The solid-state structure was solved by heavy-atom Patterson methods, and the hydrogen atoms were fixed in calculated positions with d(C−H) = 0.98 Å. All calculations were performed using the *teXsan*[30] crystallographic software package of Molecular Structure Corporation.

Data collection and structure solution for complexes **11** and **16** were conducted at Simon Fraser University. Data were recorded at ambient temperature with an Enraf Nonius CAD4F diffractometer using graphite-monochromatized Mo Kα radiation. The data were corrected for absorption by the Gaussian integration method, and corrections were carefully checked against measured ψ-scans. Data reduction included corrections for Lorentz and polarization effects and for intensity scale variation. The programs used for absorption corrections, data reduction, structure solution, and graphical output were from the *NRCVAX* Crystal Structure System.[31] Full matrix, least-squares refinement was carried out using *CRYSTALS*.[32] Complex scattering factors for neutral atoms[33] were used in the calculation of structure factors. Computations were carried out on a Pentium computer.

During the structure determination of complex **11** many hydrogen atoms were located in the electron density difference map. Although independent coordinates and isotropic temperature factors were refined for H(19) and H(22), all other hydrogen atoms were placed in calculated positions (d(C−H) = 0.95 Å) and were made to ride on their respective carbon atoms during refinement. Difference map features also suggested orientational disorder of four of the Cp*-methyl groups. These features were flattened by inclusion of two mutually staggered CH$_3$ orientations of complementary partial occupancies (totalling 1) for each of these four methyl groups. In each case the entire disordered methyl-ensemble was then refined as a rigid group, with a relative occupancy parameter for the two orientations, subject to restraints which kept each CCH$_3$ fragment axially symmetric. A single parameter was refined for the isotropic displacement of the hydrogen atoms of each saturated CH, CH$_2$, and CH$_3$ group and the hydrogen atoms (other than H(22)) of the phenyl group, and the shifts were applied to the individual hydrogen atom values.

Many hydrogen atoms were located in an electron density difference map during the solution of the structure of complex **16**, in particular those bonded to the vinylic carbon atom C(20). The coordinates of the hydrogen atoms bonded to C(20) were refined independently. All other hydrogen atoms were placed in calculated positions (d(C−H) = 0.95 Å) and were made to ride on their respective carbon atoms during refinement. Isotropic thermal parameters for the hydrogen atoms were initially assigned proportionately to the equivalent isotropic thermal parameters of their respective carbon atoms. Subsequently the isotropic thermal parameters for each of the following groups of hydrogen atoms were constrained to have identical shifts during refinement: those of the Cp* group, the methylene group, the SiMe$_3$ ligand, the PMe$_3$ substituent, the vinyl ligand, and the phenyl substituent.

Kinetic Studies. Kinetic studies were performed using gastight quartz cells and an HP8452 UV−vis spectrometer equipped with a thermostated cell holder connected to a VWR1150 constant-temperature bath, which was accurate to ±0.05 °C. At least two replicate kinetic runs were employed in the determination of k_{obs} for a given set of experimental conditions. Typical kinetic runs monitored the product band at 350 or 360 nm arising from the thermolysis of 0.1−1 mg of **1** or **5** dissolved in 3 mL of solvent over not less than 3.5 half-lives. Absorbance values for t_∞ were obtained by optimization of the squared residual, R^2, for the regression line fitted to the data through a first-order analysis.

Competition Experiments. A sample of Cp*W(NO)(CH$_2$SiMe$_3$)(η^2-CPhCH$_2$) (8 mg, 15 μmol) was dissolved in a 1:1 (mol:mol) mixture of the appropriate solvents (0.5 mL) which was prepared by weighing equimolar volumes of solvent into a vial prior to addition of the solid organometallic reagent. The resulting solution was heated at 54 °C in an NMR tube equipped with a Rotaflo Teflon valve. After 1 h the volatiles were removed under vacuum, C$_6$D$_6$ was added, and the ^{1}H NMR spectrum was recorded utilizing relaxation delays in excess of 90 s to ensure full relaxation of all proton environments prior to excitation. The ratios of products were determined by multiple integration of the appropriate vinyl and/or methyl signals. The absolute errors in these integrations were assumed to be 5%. The per-C−H-bond selectivities were calculated analogously, but the amount of each species was corrected for the number of symmetry-equivalent C−H bonds in each case.

Equilibration of Cp*W(NO)(R^2)(CPhCH$_2$) and Cp*W(NO)(R^1)(CPhCH$_2$). Solutions of Cp*W(NO)(CH$_2$SiMe$_3$)(η^2-CPh=CH$_2$) (8 mg, 15 μmol), dissolved in a 1:1 (mol:mol) mixture (0.5 mL) of the appropriate solvents as in the previous case, were heated at 54 °C in an NMR tube equipped with a Rotaflo Teflon valve. After 96 h the volatiles were removed under vacuum, the residue was dissolved in C$_6$D$_6$, and the ^{1}H NMR spectrum was recorded. The equilibrium constant K_{eq}(327 K) was determined in each case as the ratio [Cp*W(NO)(R^2)(CPhCH$_2$)]/[Cp*W(NO)(R^1)(CPhCH$_2$)]. A single-point calculation utilizing $\Delta G°(327\ K) = -RT\ \ln(K_{eq})$ afforded approximate values of the equilibrium free energy for each of the equilibria. Additionally, the amounts of Cp*W(NO)(R^2)(CPh

(29) Legzdins, P.; Rettig, S. J.; Ross, K. J.; Batchelor, R. J.; Einstein, F. W. B. *Organometallics* **1995**, *14*, 5579.

(30) *teXsan* Crystal Structure Analysis Package; Molecular Structure Corporation, 1985 & 1992.

(31) Gabe, E. J.; LePage, Y.; Charland, J.-P.; Lee, F. L.; White, P. S. *J. Appl. Crystallogr.* **1989**, *22*, 384.

(32) Watkin, D. J.; Carruthers, J. R.; Betteridge, P. W. *CRYSTALS*, Chemical Crystallography Laboratory, University of Oxford: Oxford, England, 1995.

(33) Cromer, D. T.; Waber, J. T. *International Tables for X-ray Crystallography*; Kynoch Press: Birmingham, England, 1975; Vol. IV, p 99.

CH_2) and Cp*W(NO)(R^1)($CPhCH_2$) were corrected for the number of symmetry-equivalent C−H bonds in each case, thereby yielding the per-C−H-bond equilibrium expression.

Thermolyses of Cp*W(NO)($CPhCH_2$)(CH_2SiMe_3) (1) in Hydrocarbon Solvents. The thermolyses of complex **1** in various solvents were performed in a similar manner throughout. Compounds **2**−**10** crystallize readily from hydrocarbon or ethereal solvents and may be isolated in yields ranging from 70 to 85%. The preparation of **2** via the thermolysis of **1** in benzene is described as a representative example.

In an inert atmosphere glovebox, a thick-walled glass bomb was charged with **1** (135 mg, 0.25 mmol). The bomb was removed from the glovebox and connected to an inert atmosphere/vacuum line, whereupon benzene (ca. 5 mL) was vacuum transferred onto the crystalline solid cooled to −196 °C. Warming of the bomb to room temperature yielded a burgundy solution of **1**. The bomb was then placed in a constant-temperature oil-bath and maintained at 54 °C for 24 h, during which time the solution lightened in color to a deep red-brown. When the thermolysis was deemed to be complete, the bomb was removed from the bath and cooled to room temperature. The solvent was subsequently removed under high vacuum, and the remaining oily solids were maintained under high vacuum for 1 h. After this time the bomb was taken into the inert-atmosphere glovebox and the contents were dissolved in a minimum of diethyl ether. The resulting red-brown solution was filtered through a column of Celite (0.5 × 3.0 cm), the column was rinsed with diethyl ether (1 × 1 mL), and the filtrate was concentrated in vacuo. Cooling of the filtrate for 24 h at −30 °C resulted in the deposition of analytically pure **2** as red-brown blocks. Complexes **3m**, **3p**, and **9** were prepared in an analogous manner.

Preparation of 5, 10, and Metallacycles 11−**15.** These compounds were prepared in a manner analogous to that described for the preparation of **2** above by employing the appropriate solvent. However, in each case the ether extract was passed through alumina I instead of Celite. Concentration and cooling of the yellow-orange eluates afforded analytically pure, crystalline solids in each case. Complexes **11**, **12**, **14**, and **15** were recrystallized from 1:1 Et_2O/hexanes, hexanes, 1:1 Et_2O/hexanes, and Et_2O, respectively.

Preparation of Xylyl Complexes 6 and 7. These complexes were prepared in a manner analogous to that employed for the synthesis of **2**. Concentration and cooling of the diethyl ether filtrate resulted in the cocrystallization of **6** and **7** as red-brown irregular blocks. In an independent preparation, benzyl complex **7** was isolated as analytically pure red crystals by concentration and cooling of the Et_2O eluate that resulted from passing an extracted mixture of **6** and **7** through a column of alumina I (1 cm × 3 cm).

Independent Preparation of Benzyl Complex 4. Authentic **4** was prepared by metathetical methods employing Cp*W(NO)Cl_2 (420 mg, 1 mmol), $(CH_2{=}CPh)_2Mg{\cdot}x$(dioxane), and $(PhCH_2)_2Mg{\cdot}x$(dioxane) (210 and 155 mg, respectively, 1 equiv each). The organometallic dichloride complex and bis(phenylvinyl)magnesium were mixed in a 25 mL Erlenmeyer flask, which was subsequently immersed in a glovebox coldwell and cooled to ca. −180 °C. THF (10 mL) was added in a dropwise fashion down the sides of the flask, whereupon it froze upon contacting the cooled solids. The solid puck was allowed to warm slowly to room temperature with stirring, whereupon the solids dissolved and a burgundy-black solution resulted. The reaction mixture was cooled to −30 °C, and a cooled THF solution of the bis(benzyl)magnesium reagent (−30 °C) was added dropwise with concomitant agitation of the reaction flask. The contents were then allowed to warm to room temperature with stirring. After the reaction mixture had been stirred for 0.5 h at room temperature, the THF was removed from the mixture under vacuum, and the remaining red solids were maintained under high vacuum for 2 h. The solids were extracted with diethyl ether (35 mL), and the extracts were passed down a column of alumina I. The red band that developed was collected. Concentration of the eluate and subsequent cooling afforded **4** as a red crystalline solid (typical yields 70−75%).

Preparation of Metallacyclopropane Complex 16. Vinyl complex **1** (0.25 g, 0.464 mmol) was dissolved in hexanes, and the resulting burgundy solution was placed in a glass bomb. The solution was cooled to −196 °C, and PMe_3 (excess) was vacuum-transferred onto the frozen solids. The mixture was thawed and then stirred at room temperature for 4 h, during which time the solution changed from a burgundy to a bright yellow color and small, needlelike crystals deposited on the walls of the reaction flask. After this time, the volatiles were removed under high vacuum, and the yellow residue was then dissolved in dichloromethane (5 mL). Hexanes (10 mL) were added, and the solution was placed in a freezer (−30 °C) to induce crystallization. Compound **16** was isolated as yellow crystals by removing the supernatant liquid via cannulation.

Acknowledgment. We are grateful to the Natural Sciences and Engineering Research Council of Canada for support of this work in the form of grants to P.L. and a postgraduate fellowship to S.A.L. We also thank The University of British Columbia for the award of a University Graduate Fellowship to S.A.L., and we acknowledge Dr. P. J. Daff for stimulating and helpful discussions.

Supporting Information Available: Tables listing crystallographic information, atomic coordinates and B_{eq}, anisotropic thermal parameters, and intramolecular bond distances, angles, and torsion angles. This material is available free of charge via the Internet at http://pubs.acs.org.

OM9904450